Loss of multi-level 3D genome organization during breast cancer progression

Supplemental Figures

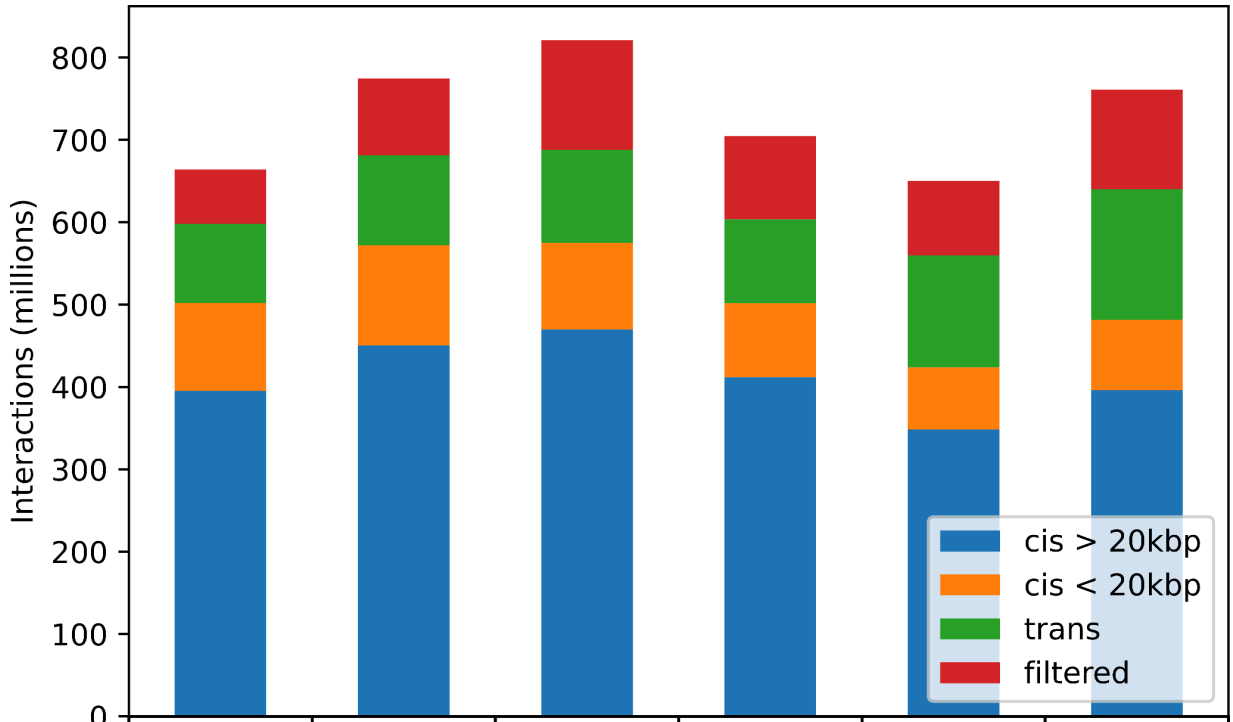

	MCF10A rep.1	MCF10A rep.2	MCF10AT1 rep.1	MCF10AT1 rep.2	MCF10CA1a rep.1	MCF10CA1a rep.2
cis > 20kbp	395.19	450.37	469.72	411.8	348.31	396.13
cis < 20kbp	106.91	121.64	105.22	89.85	75.64	85.27
trans	95.93	109.5	112.73	101.96	135.7	158.56
filtered	66.14	92.97	133.61	101.12	90.5	120.95
total	664.17	774.48	821.28	704.73	650.15	760.91

Fig. S1: Barplot showing the number of Hi-C interactions (in millions) classified by type: long-range cis (blue), short-range cis (orange), trans (green) and filtered out (red). The table under the graph shows the data underlying the barplot.

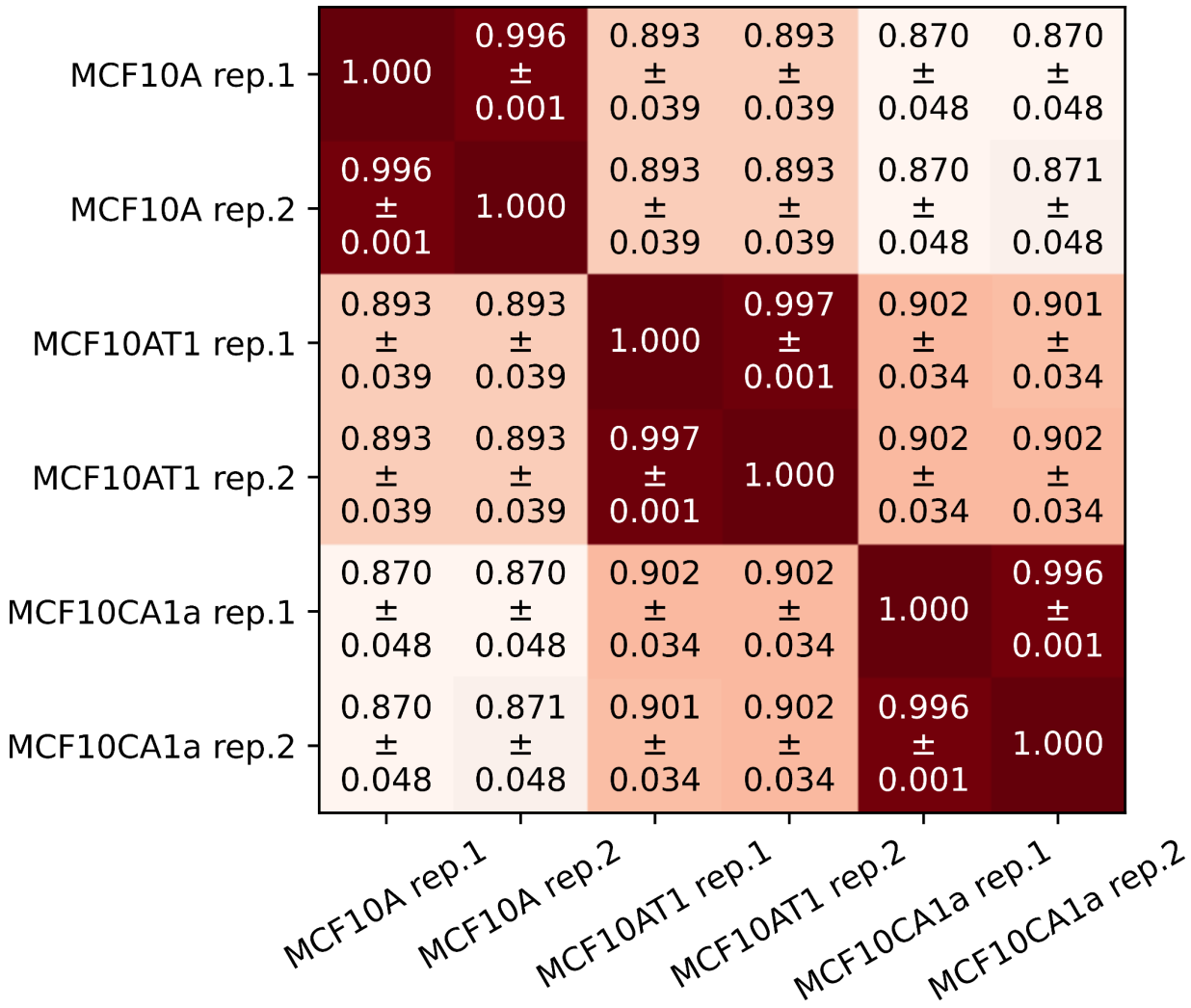

Fig. S2: Heatmap showing the weighted average of the stratified correlation coefficient (SCC) computed for each pair of samples using HiCRep, which avoids inflated correlations from distance-dependent decay in HiC data. Chromosome sizes are used as weights in the computation of the SCC weighted average. Overlaid numbers show the weighted average and standard deviation for each pair of samples.

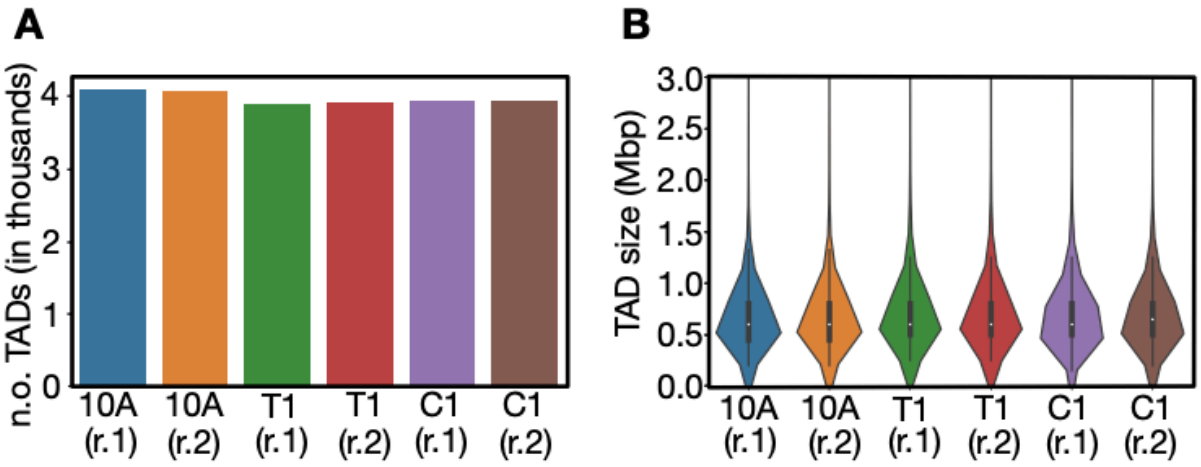

Fig. S3: **A**: Number of TADs (in thousands) for each of the six Hi-C samples generated. **B**: Comparison of genomic sizes of all TADs for the six samples.

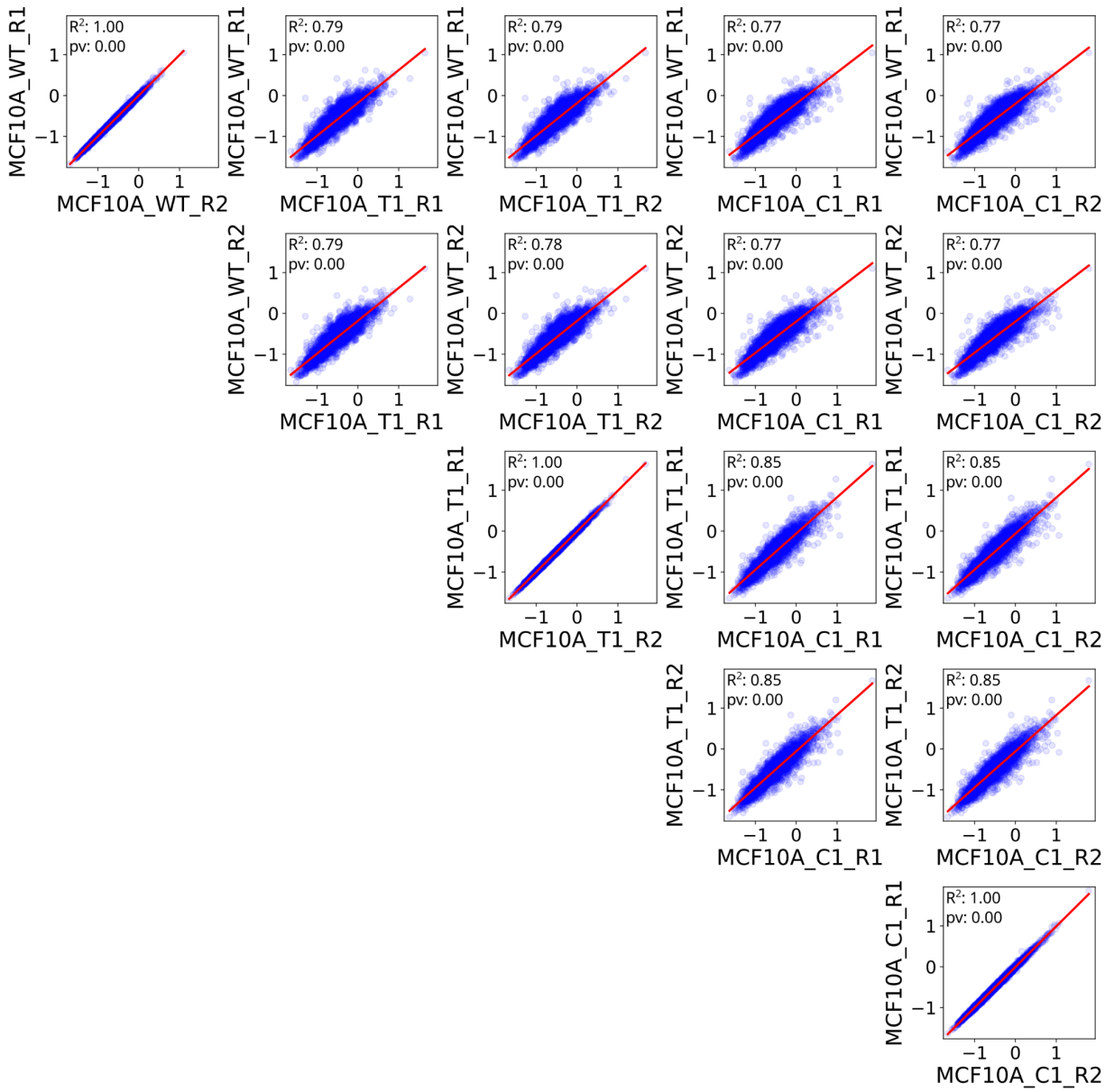

Fig. S4: Scatterplot contrasting TAD insulation scores at 50 kbp resolution for all possible pairs of samples. Trend line is depicted in red.

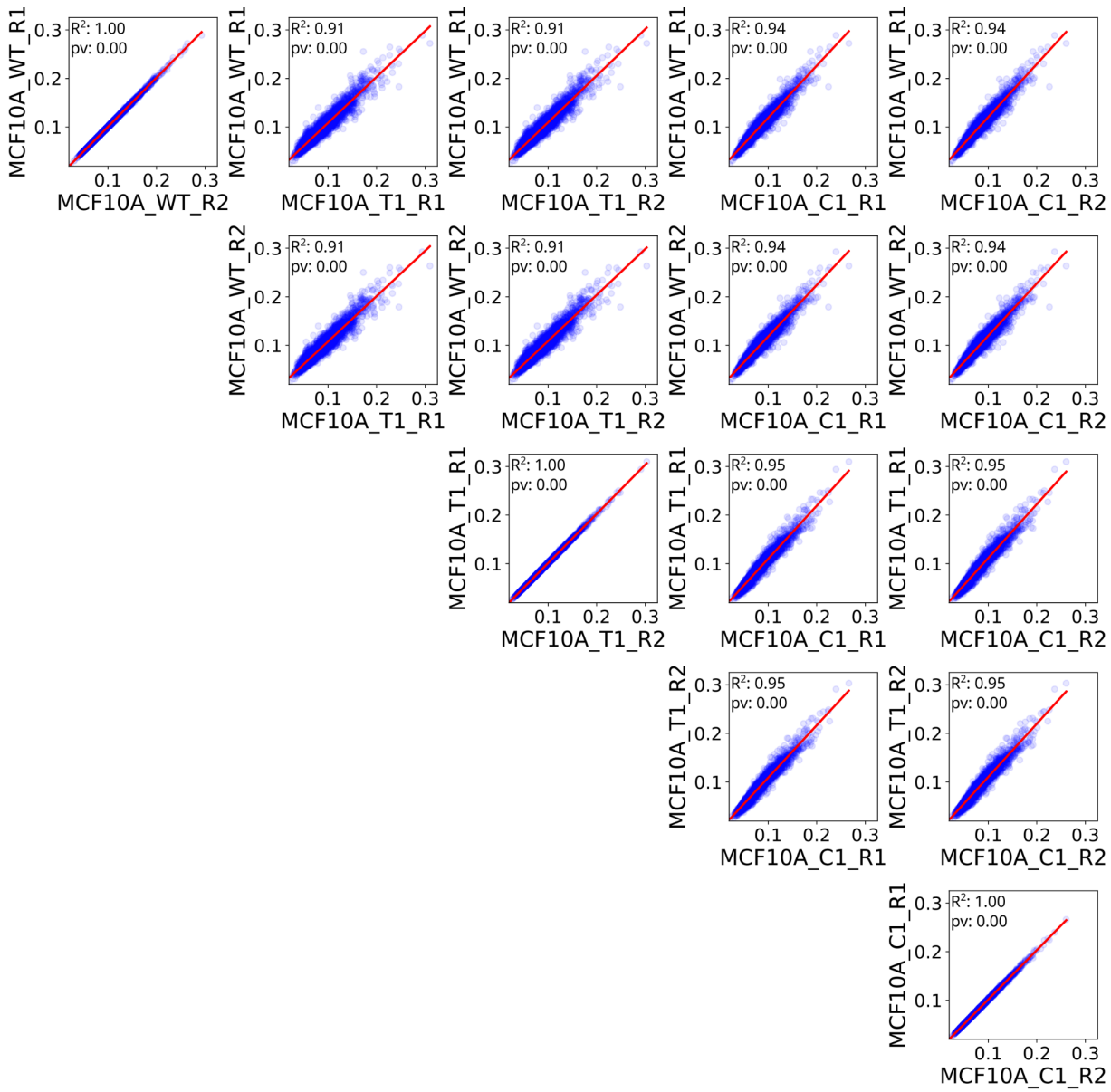

Fig. S5: Scatterplot contrasting the normalized number of interactions of MCF10A TADs at 50 kbp resolution across all possible pairs of samples. Trend line is shown in red. Scores are computed by aggregating interactions from the upper triangle of the Hi-C matrix overlapping TADs. Aggregated interactions are normalized based on the number of pixels belonging to a TAD.

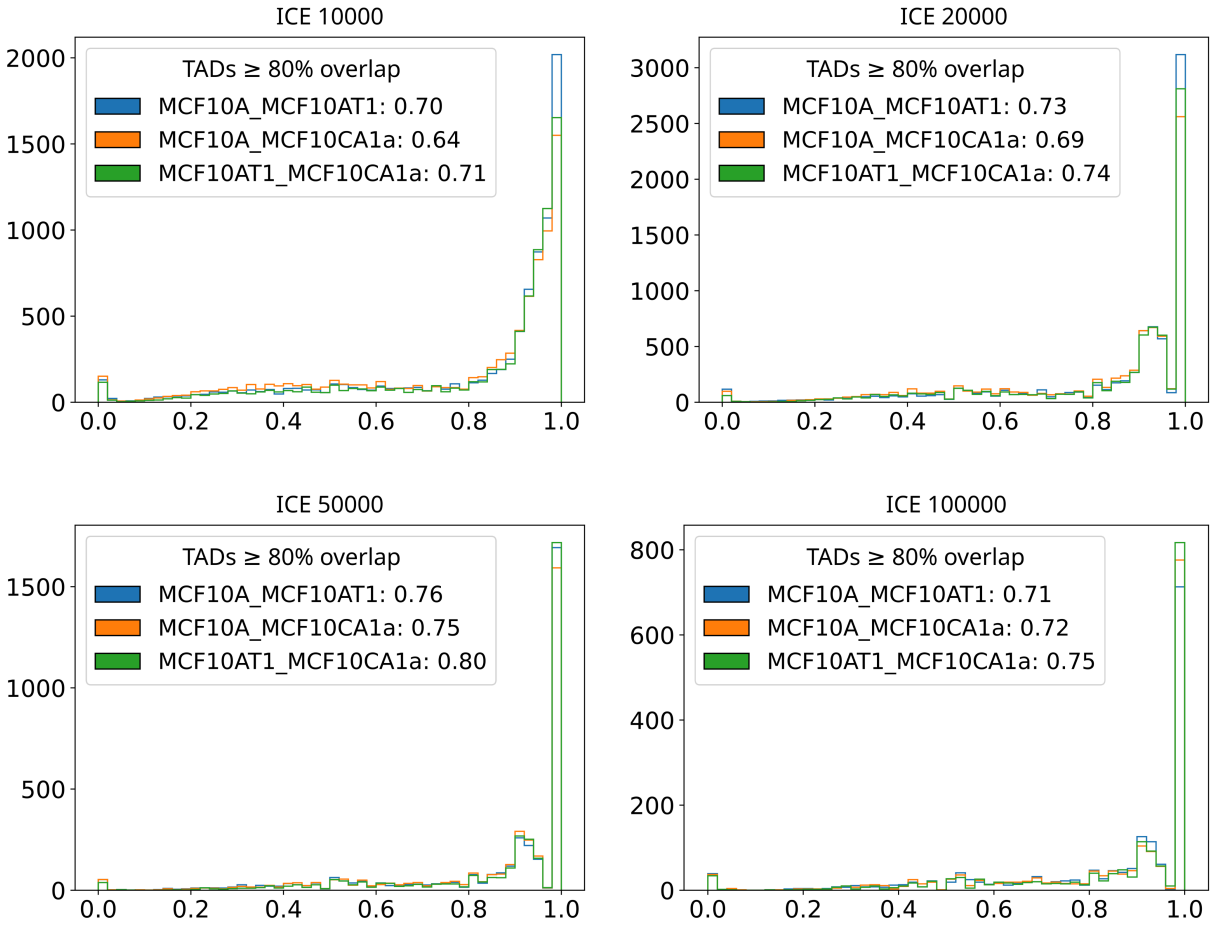

Fig. S6: Histogram of TAD Jaccard overlap coefficients. Coefficients are computed from Hi-C matrices after collapsing replicates. Numbers shown in plot legends show the fraction of TADs with at least 80% overlap. Panels show coefficients computed using TADs called at 10 kbp (top left), 20 kbp (top right), 50 kbp (bottom left) and 100 kbp (bottom right) resolutions.

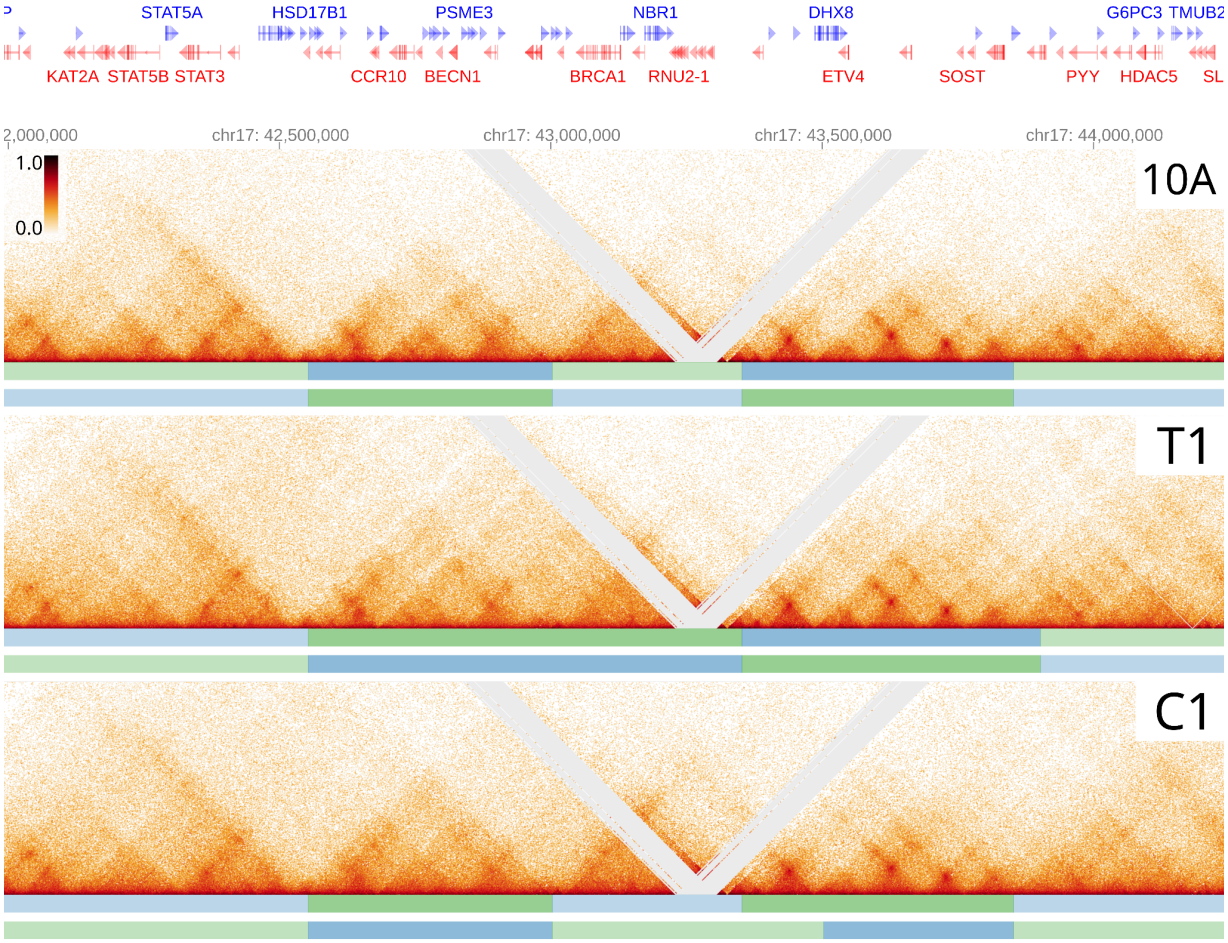

Fig S7: HiGlass view of the Hi-C matrices for 10A, T1, and C1 (replicates merged) centered around the *BRCA1* gene. Bars shown below the Hi-C matrices show the TADs called from repl. 1 and repl. 2 of the respective dataset.

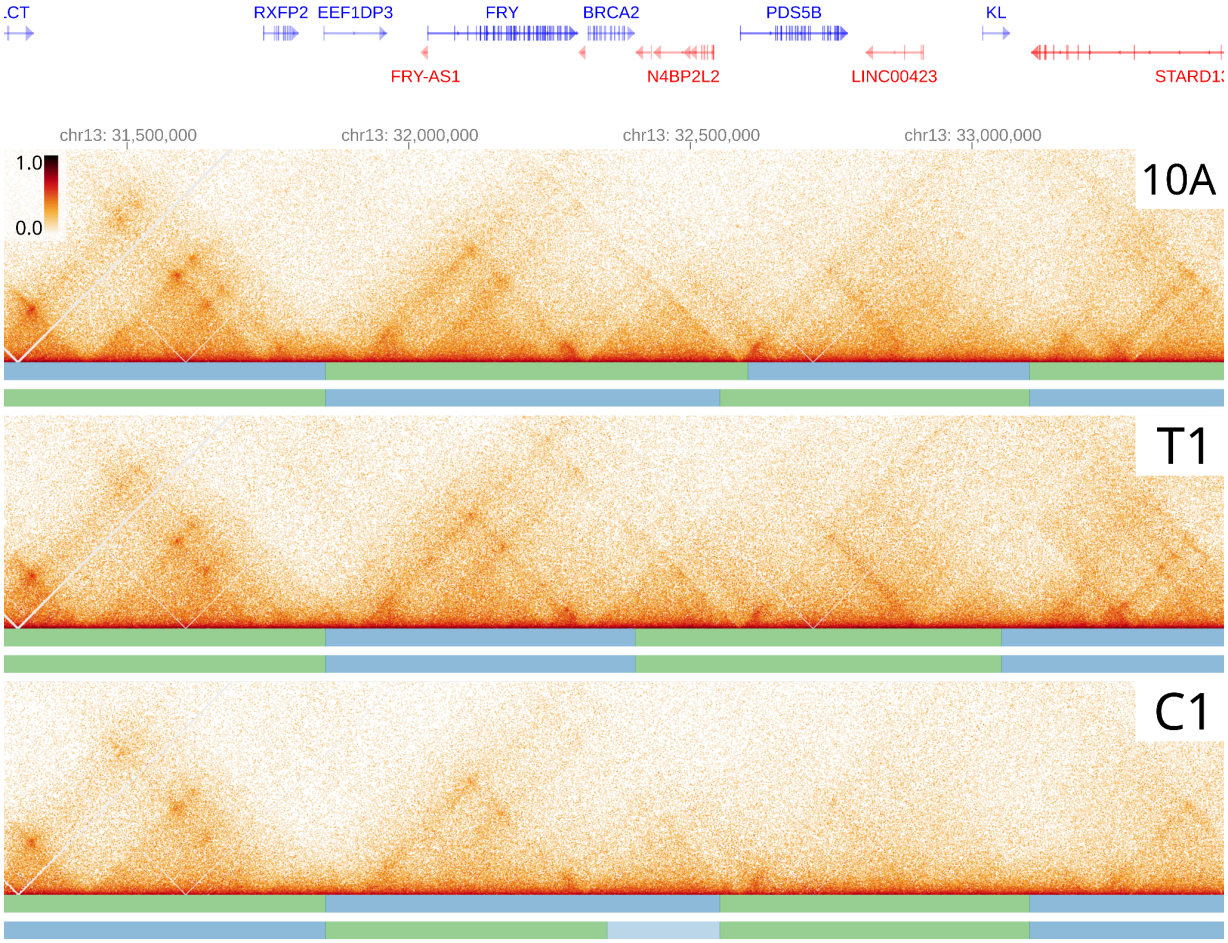

Fig S8: HiGlass view of the Hi-C matrices for 10A, T1, and C1 (replicates merged) centered around the *BRCA2* gene. Bars shown below the Hi-C matrices show the TADs called from repl. 1 and repl. 2 of the respective dataset.

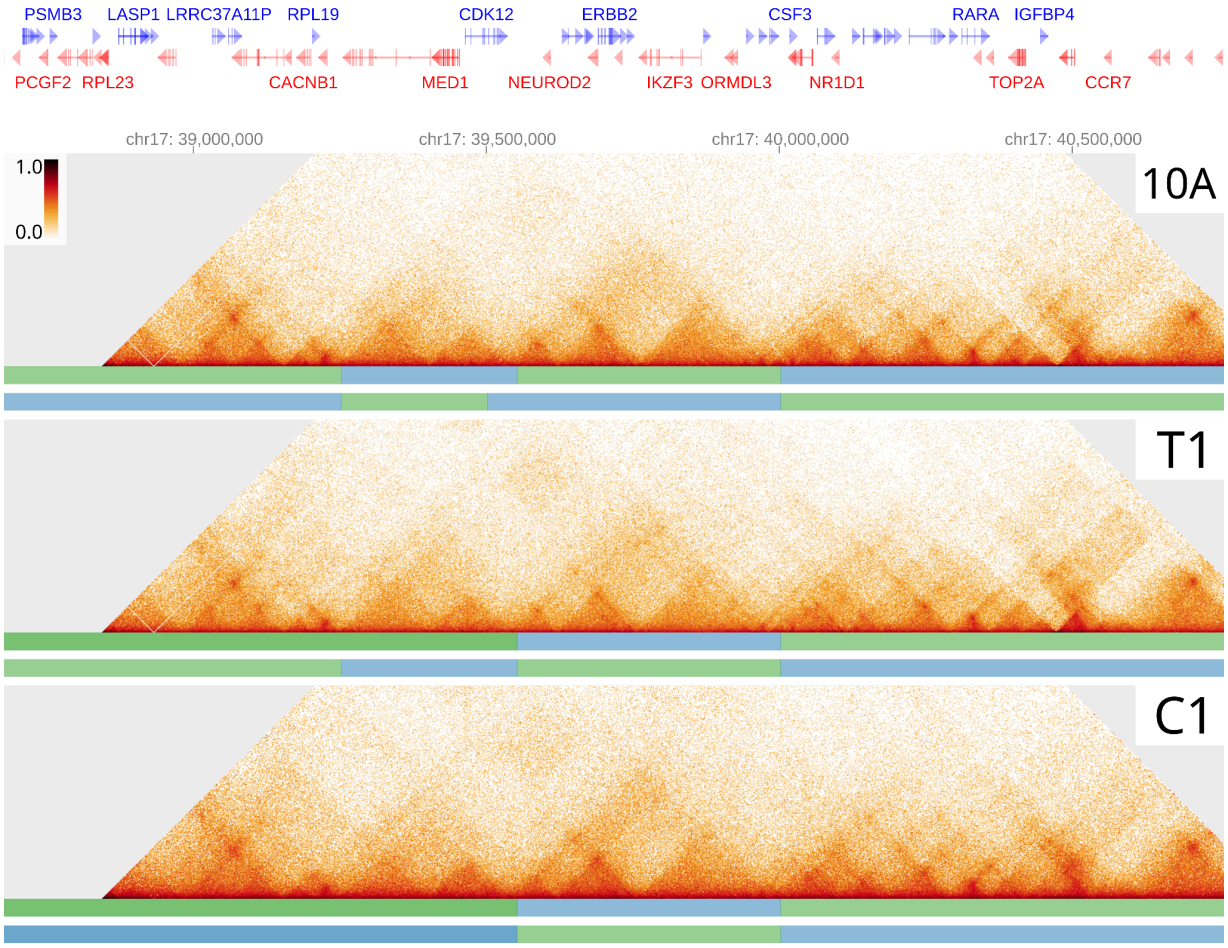

Fig S9: HiGlass view of the Hi-C matrices for 10A, T1, and C1 (replicates merged) centered around the *ERBB2* gene. Bars shown below the Hi-C matrices show the TADs called from repl. 1 and repl. 2 of the respective dataset.

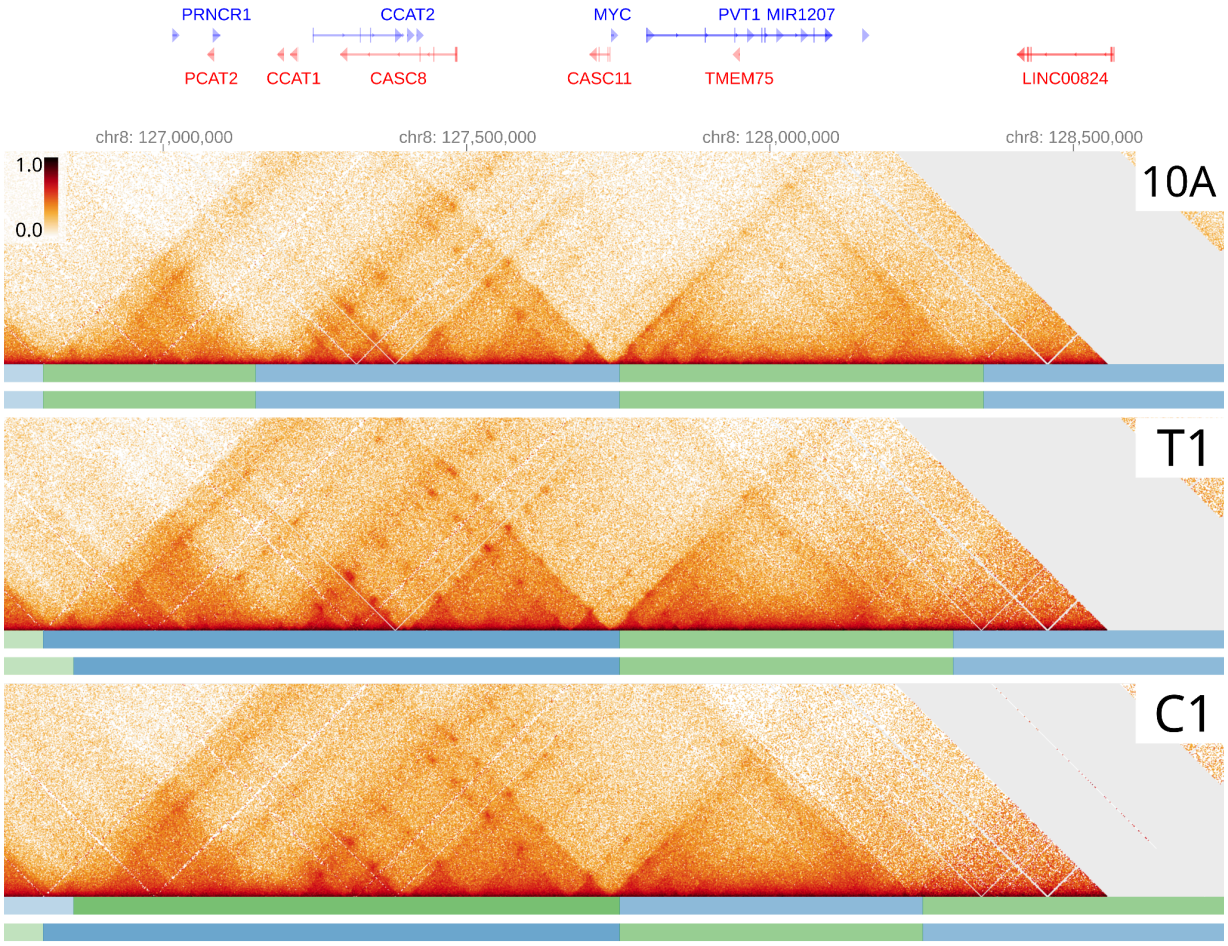

Fig S10: HiGlass view of the Hi-C matrices for 10A, T1, and C1 (replicates merged) centered around the *MYC* gene. Bars shown below the Hi-C matrices show the TADs called from repl. 1 and repl. 2 of the respective dataset.

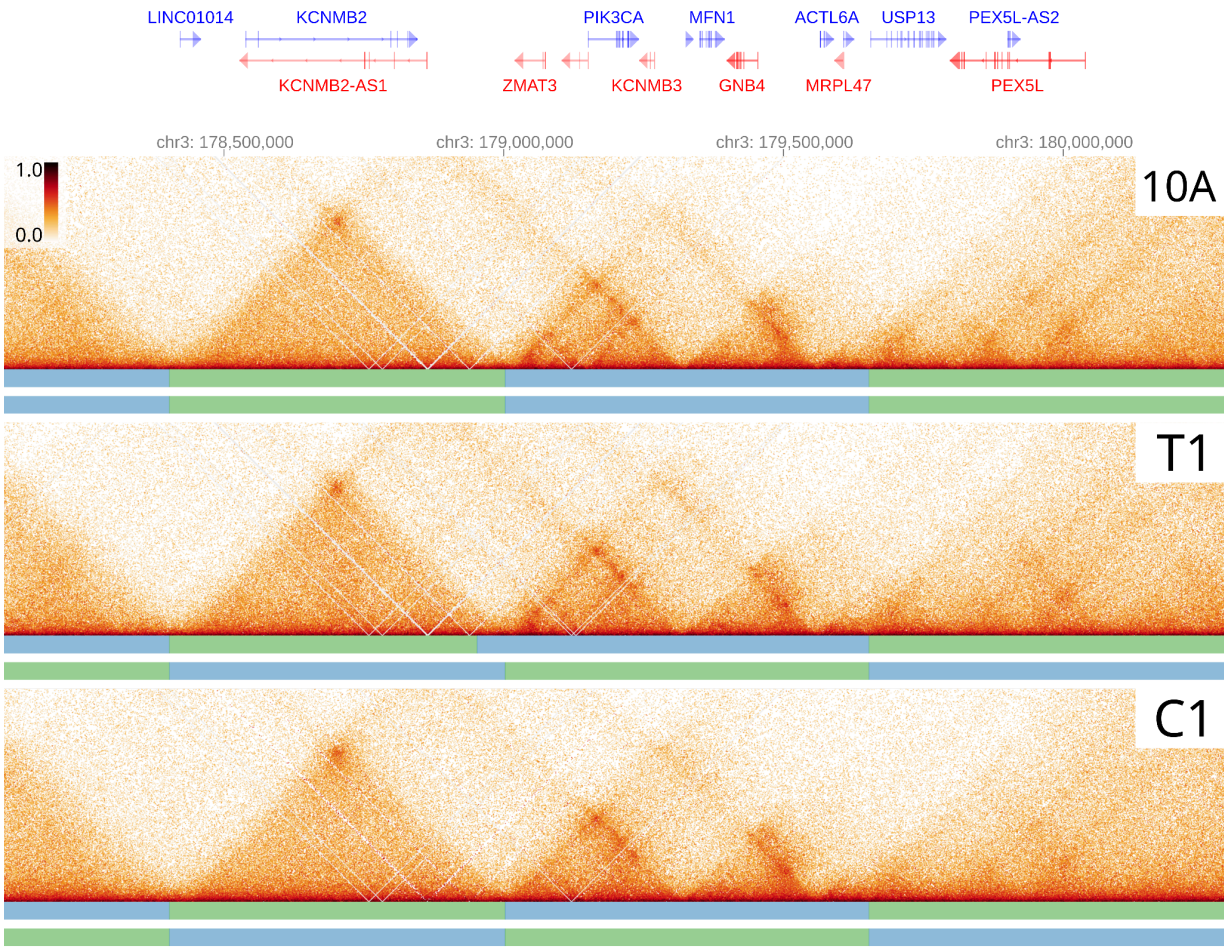

Fig S11: HiGlass view of the Hi-C matrices for 10A, T1, and C1 (replicates merged) centered around the *PIK3CA* gene. Bars shown below the Hi-C matrices show the TADs called from repl. 1 and repl. 2 of the respective dataset.

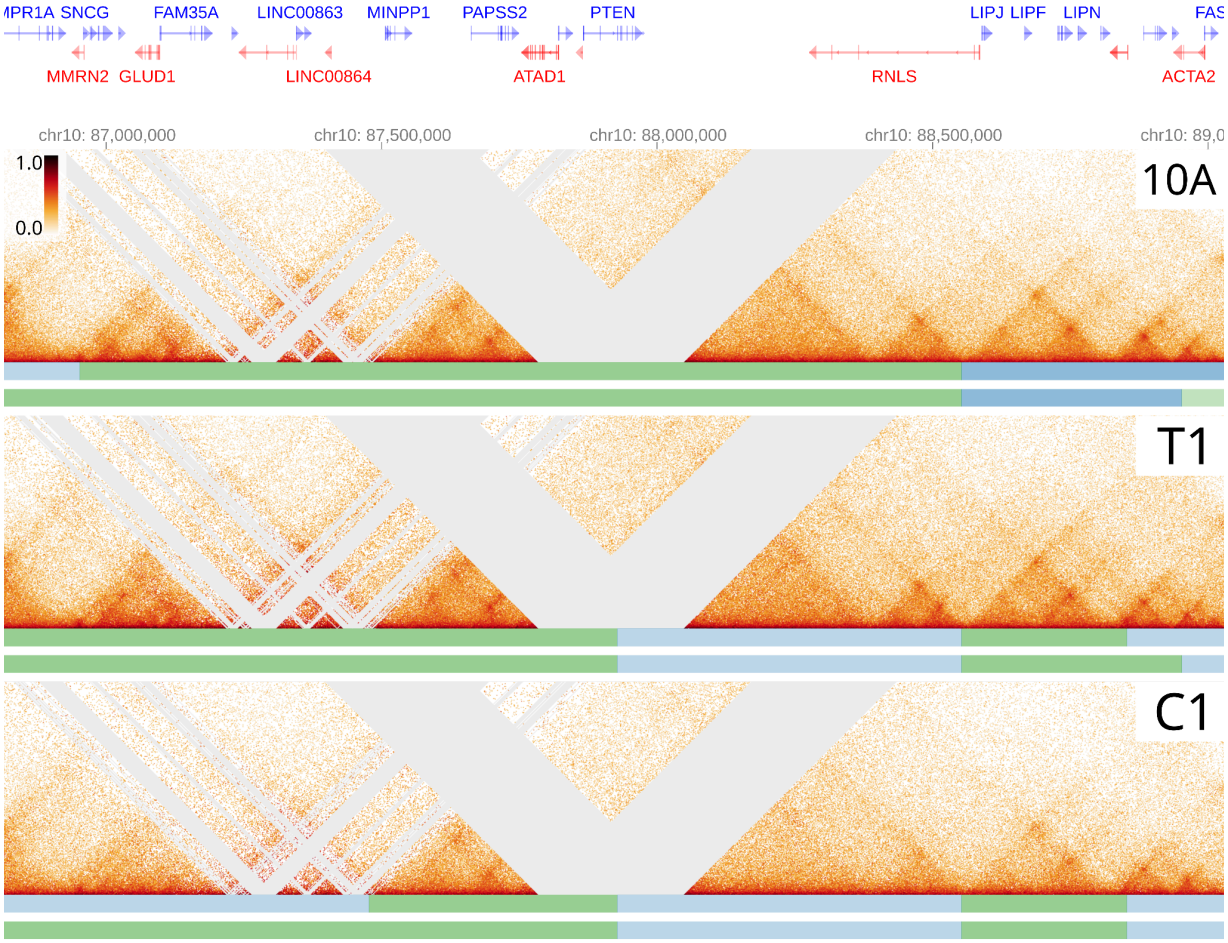

Fig S12: HiGlass view of the Hi-C matrices for 10A, T1, and C1 (replicates merged) centered around the *PTEN* gene. Bars shown below the Hi-C matrices show the TADs called from repl. 1 and repl. 2 of the respective dataset.

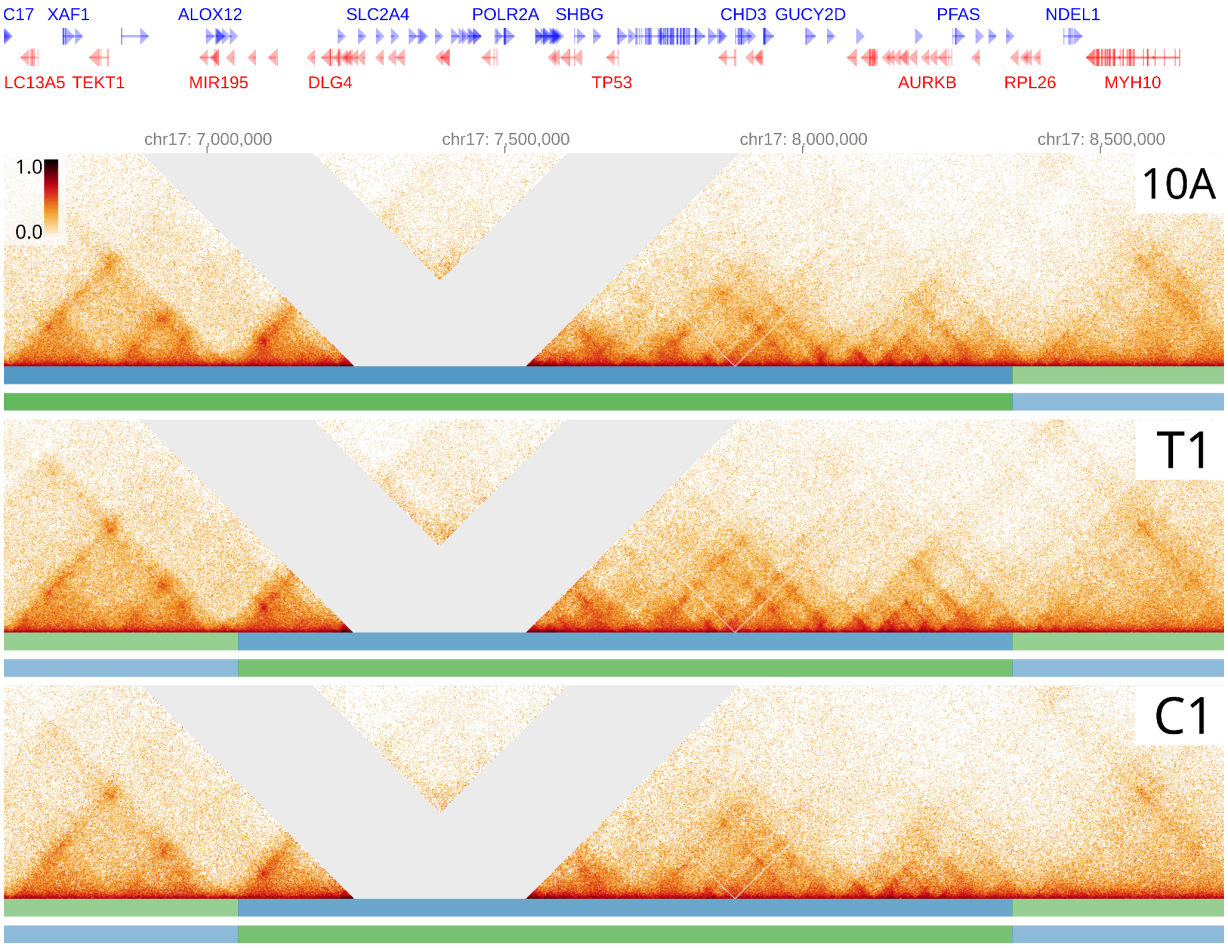

Fig S13: HiGlass view of the Hi-C matrices for 10A, T1, and C1 (replicates merged) centered around the *TP53* gene. Bars shown below the Hi-C matrices show the TADs called from repl. 1 and repl. 2 of the respective dataset.

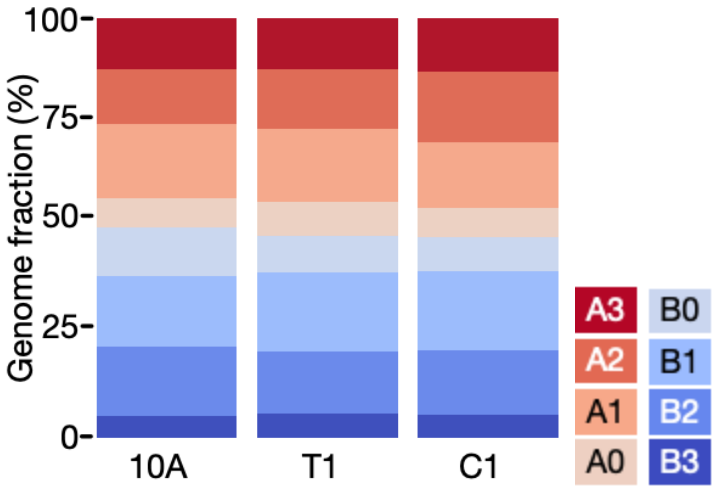

Fig. S14: Relative genome coverage of subcompartments (at 10 kbp resolution) in the three samples.

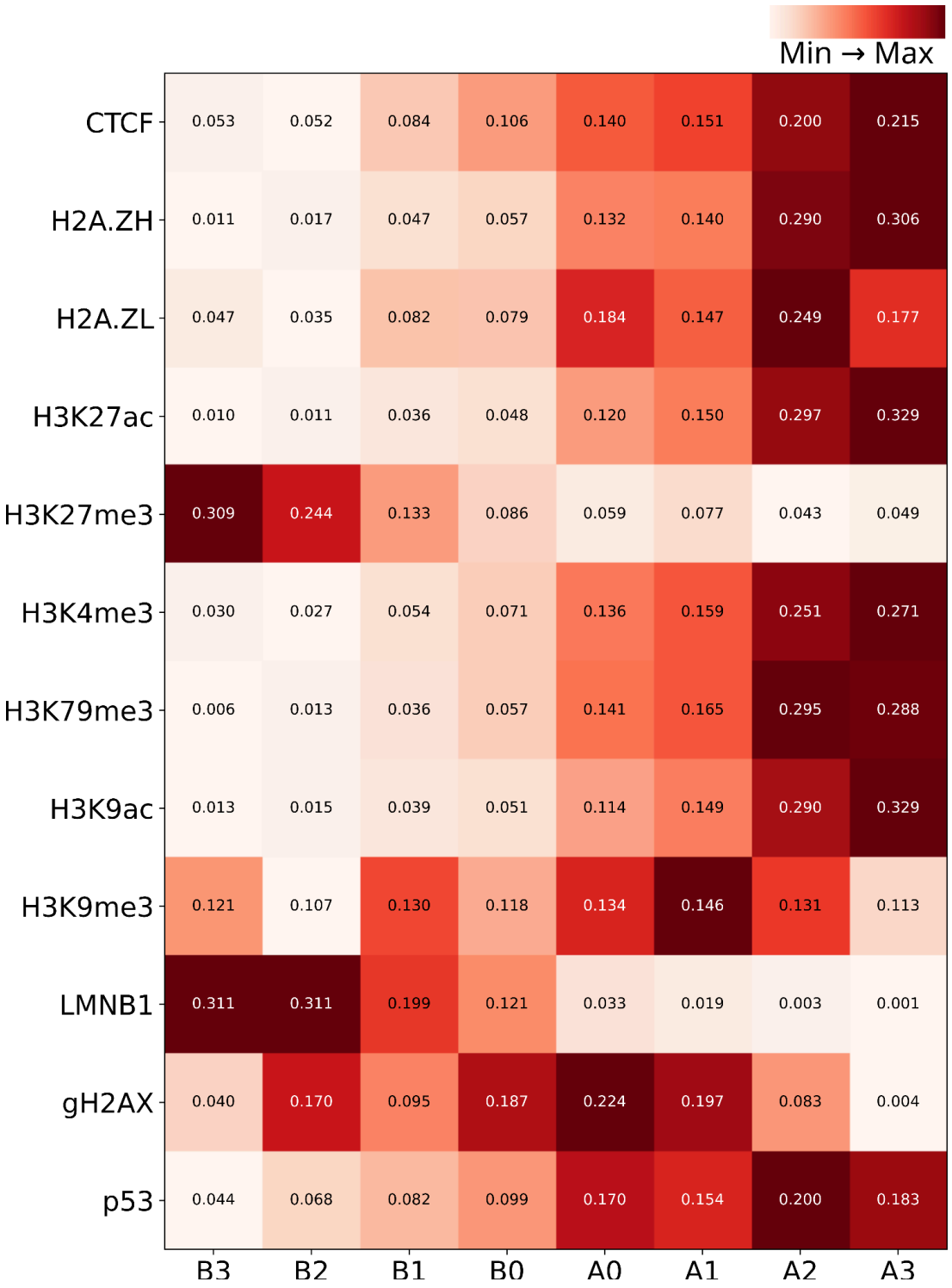

Fig. S15. Heatmap showing the average coverage of several epigenetic marks across subcompartments called on MCF10A matrices after collapsing replicates at 10 kbp resolution. Values overlaid on the heatmap show the average intensity of ChIP-seq signal over peaks overlapping each subcompartment. Color scale is normalized separately for each row to show the lowest and highest values of each row in white and dark red respectively.

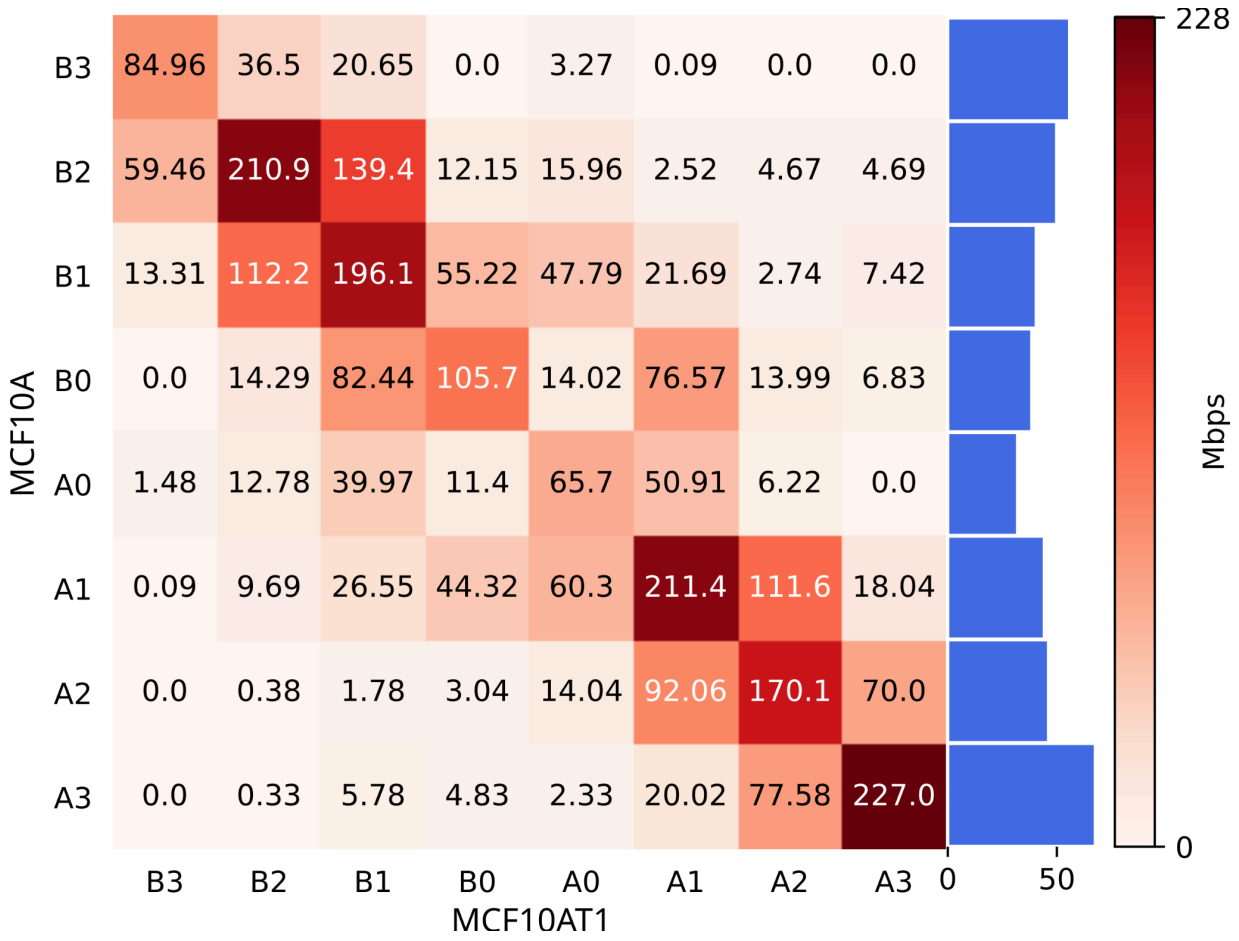

Fig. S16: Subcompartment switches (10kbp resolution) for MCF10A (WT) (vertical axis) vs MCF10AT1 (T1) (horizontal axis). Numbers are expressed in Mbp unless otherwise specified. Subcompartment switches are computed by comparing subcompartment labels across cell types. Comparison is done at the bin-level, comparing the same genomic regions.
The bar plot shows the fraction (%) of Mbps not involved in subcompartment switching. Bars are relative to the number of Mbps belonging to a given subcompartment in at least one cell type.

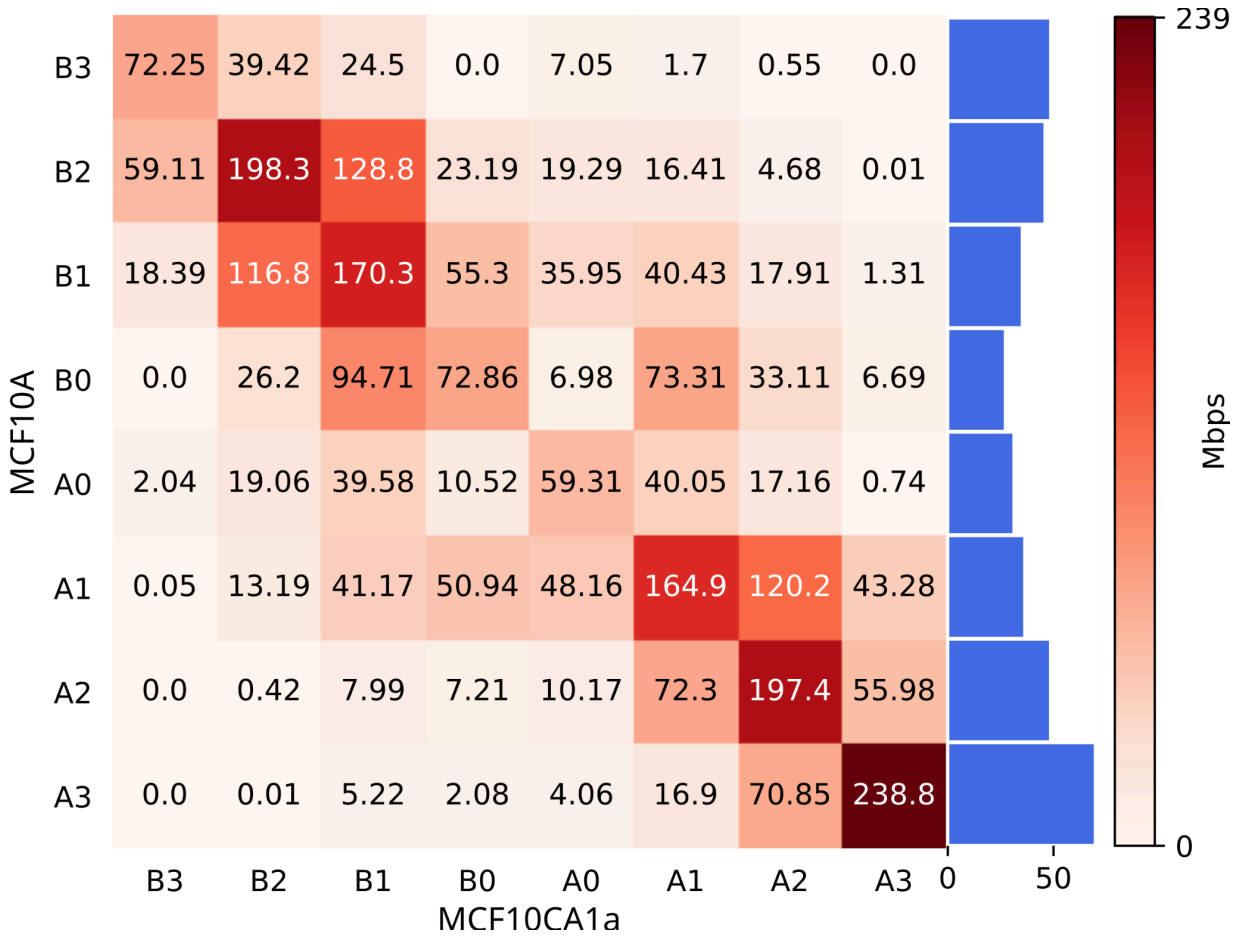

Fig. S17: Subcompartment switches (10kbp resolution) for MCF10A (WT) (vertical axis) vs MCF10CA1a (C1) (horizontal axis). Numbers are expressed in Mbp unless otherwise specified. Subcompartment switches are computed by comparing subcompartment labels across cell types. Comparison is done at the bin-level, comparing the same genomic regions. The bar plot shows the fraction (%) of Mbps not involved in subcompartment switching. Bars are relative to the number of Mbps belonging to a given subcompartment in at least one cell type.

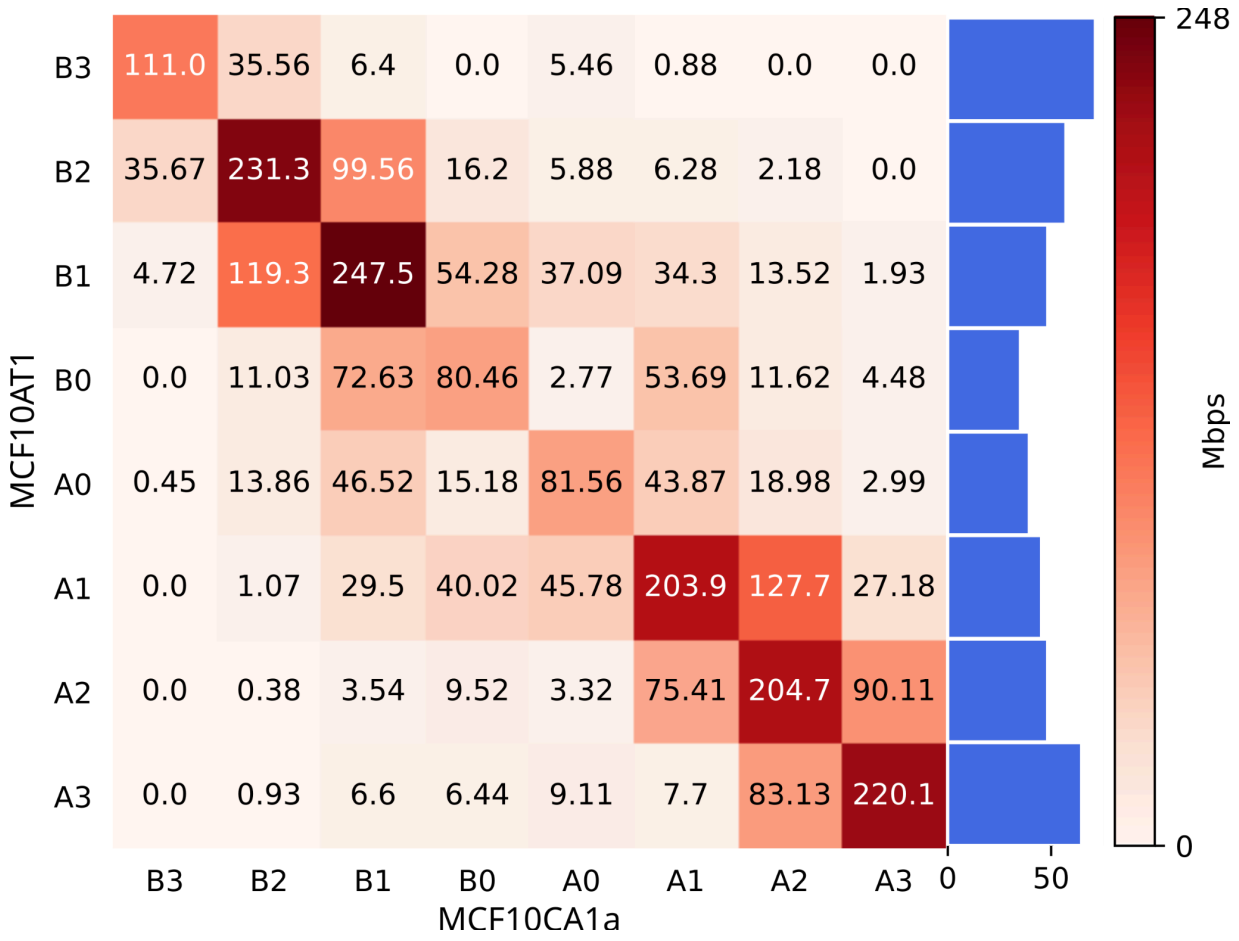

Fig. S18: Subcompartment switches (10kbp resolution) for MCF10AT1 (T1) (vertical axis) vs MCF10CA1a (C1) (horizontal axis). Numbers are expressed in Mbp unless otherwise specified. Subcompartment switches are computed by comparing subcompartment labels across cell types. Comparison is done at the bin-level, comparing the same genomic regions. The bar plot shows the fraction of Mbps not involved in subcompartment switching. Bars are relative to the number of Mbps belonging to a given subcompartment in at least one cell type.

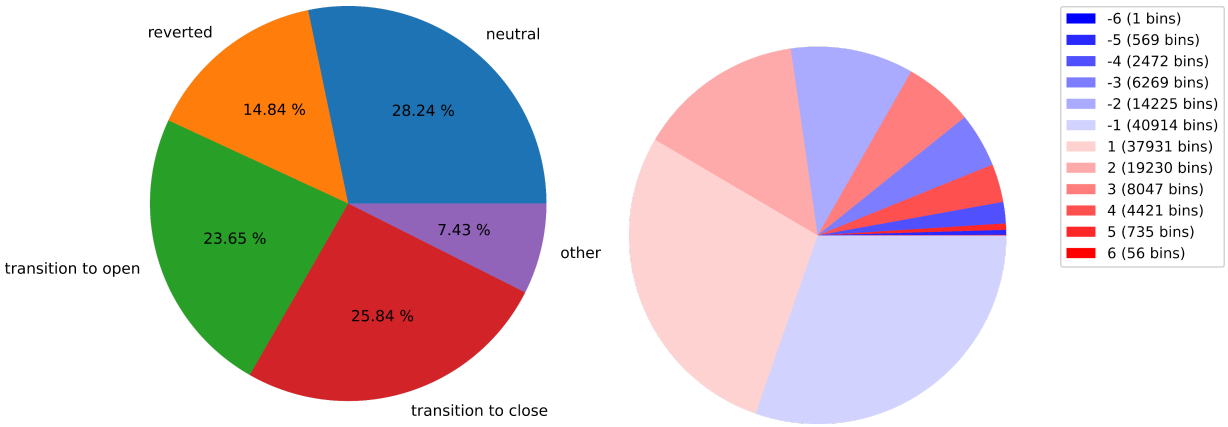

Fig. S19: Left: Pie chart showing the fate of genomic regions involved in subcompartment switches from WT via T1 to C1. Right: Pie chart showing the magnitude and direction of subcompartment switching for genomic regions involved in subcompartment switches. Positive numbers indicate a switch towards A-like subcompartments while negative values represent a switch towards B-like subcompartments. Values represent the number of consecutive subcompartment steps that are switched (e.g. A3→A0 gives a value of -3).

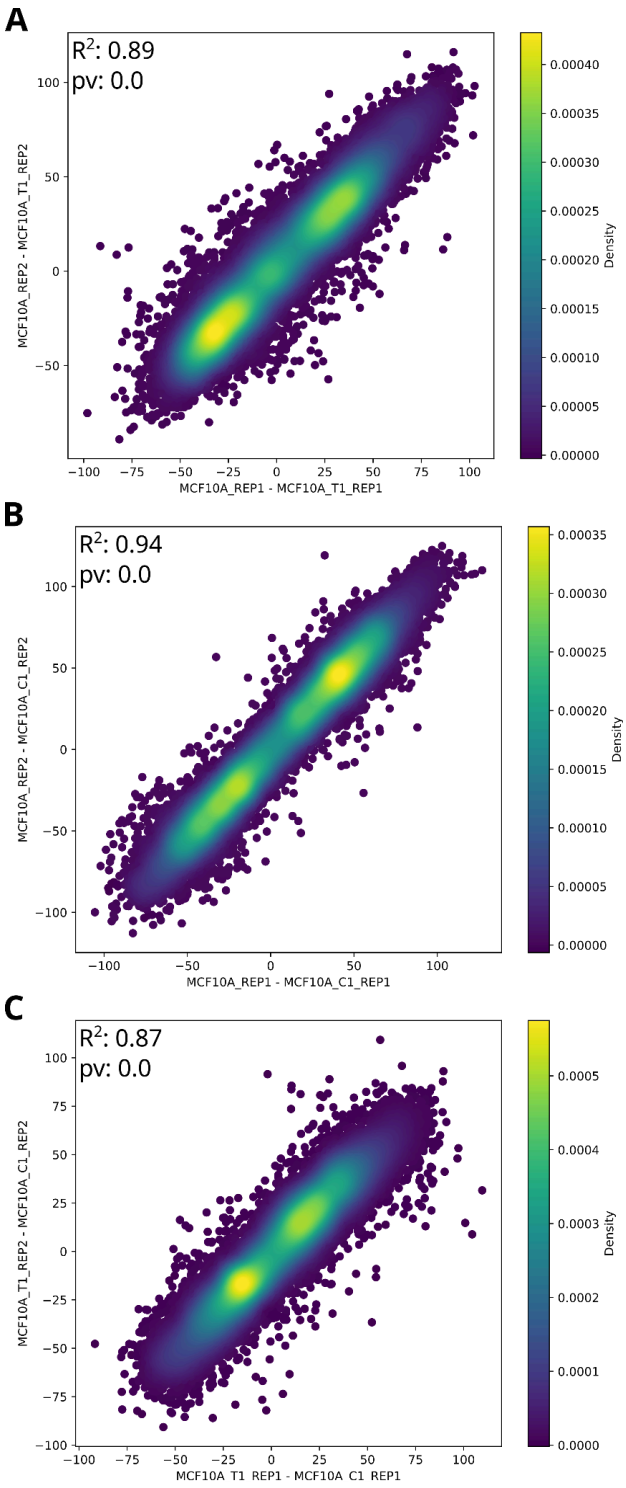

Fig. S20: Scatter plots comparing differences in compartment PCs. **A** Scatter plot comparing PC differences between 10A and T1 repl. 1 with PC differences between 10A and T1 repl. 2. **B** Scatter plot comparing PC differences between 10A and C1 repl. 1 with PC differences between 10A and C1 repl. 2. **C** Scatter plot comparing PC differences between T1 and C1 repl. 1 with PC differences between T1 and C1 repl. 2.

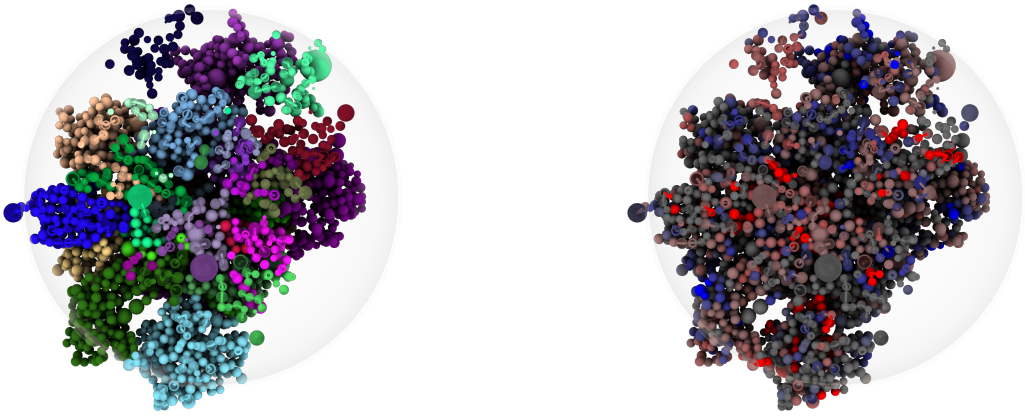

Fig S21: Left: Exemplary Chrom3D simulation model for 10A cells. Beads represent TADs sized according to genomic coverage. Chromosomes are colored distinctly. Right: The same model using sub-compartments for coloring each bead. The relative size of the model nucleus is indicated with a transparent sphere.

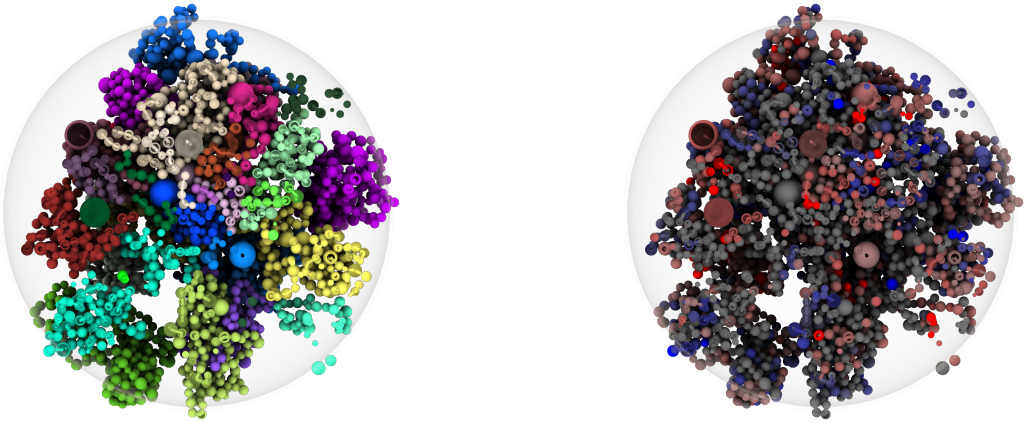

Fig S22: Left: Exemplary Chrom3D simulation model for T1 cells. Beads represent TADs sized according to genomic coverage. Chromosomes are colored distinctly. Right: The same model using sub-compartments for coloring each bead. The relative size of the model nucleus is indicated with a transparent sphere.

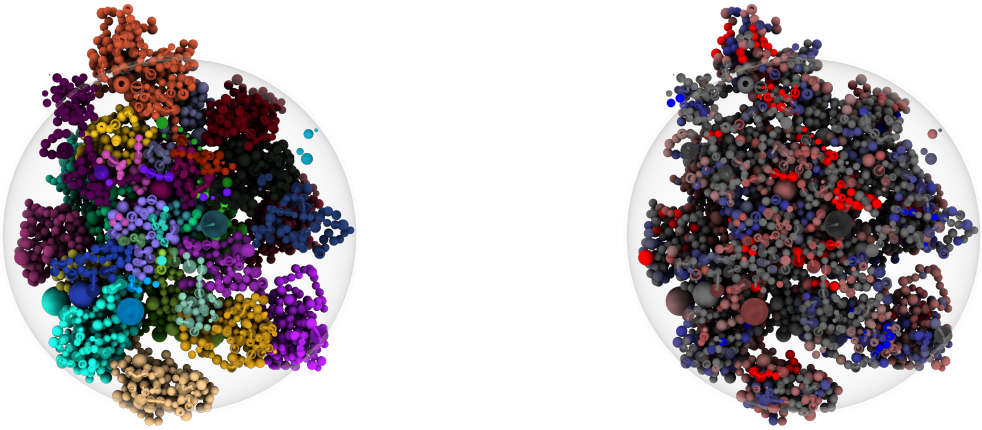

Fig S23: Left: Exemplary Chrom3D simulation model for C1 cells. Beads represent TADs sized according to genomic coverage. Chromosomes are colored distinctly. Right: The same model using sub-compartments for coloring each bead. The relative size of the model nucleus is indicated with a transparent sphere.

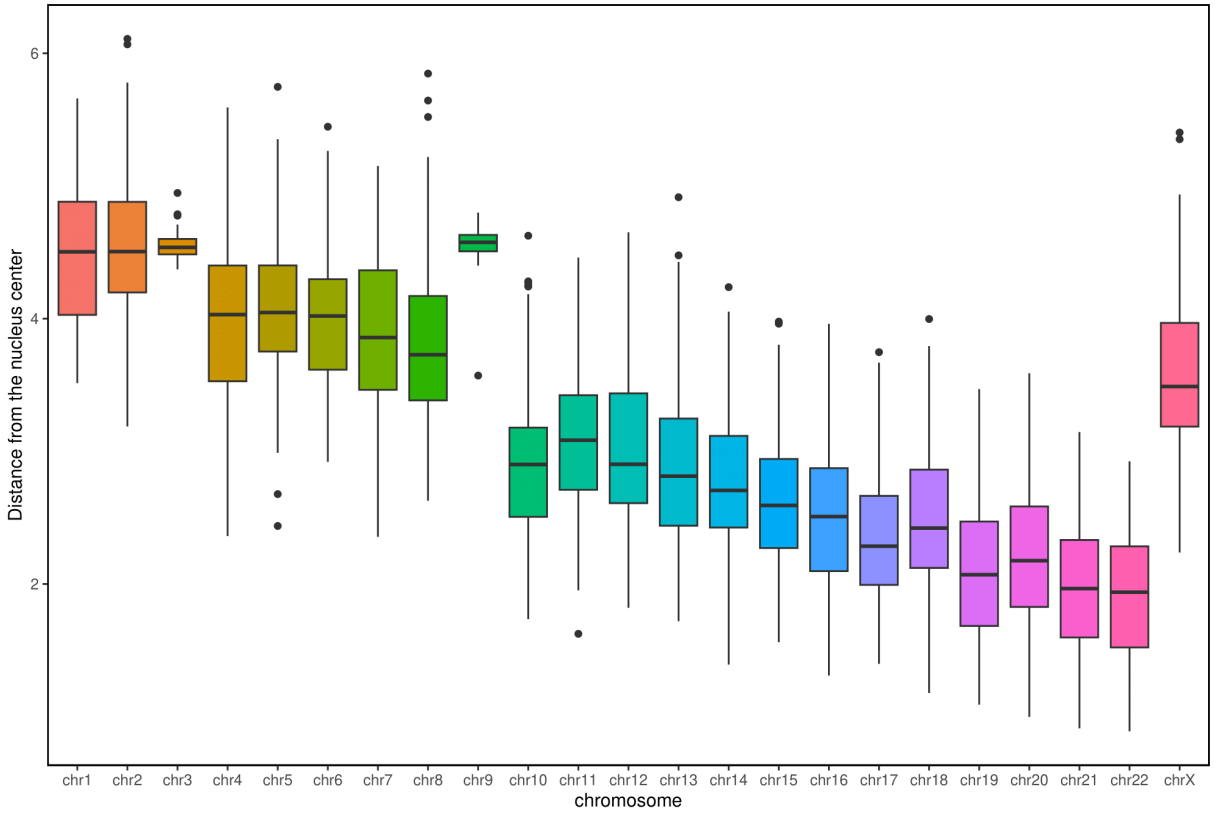

Fig. S24: Median chromosome distance from the nucleus center in 100 Chrom3D simulation models based on 10A.

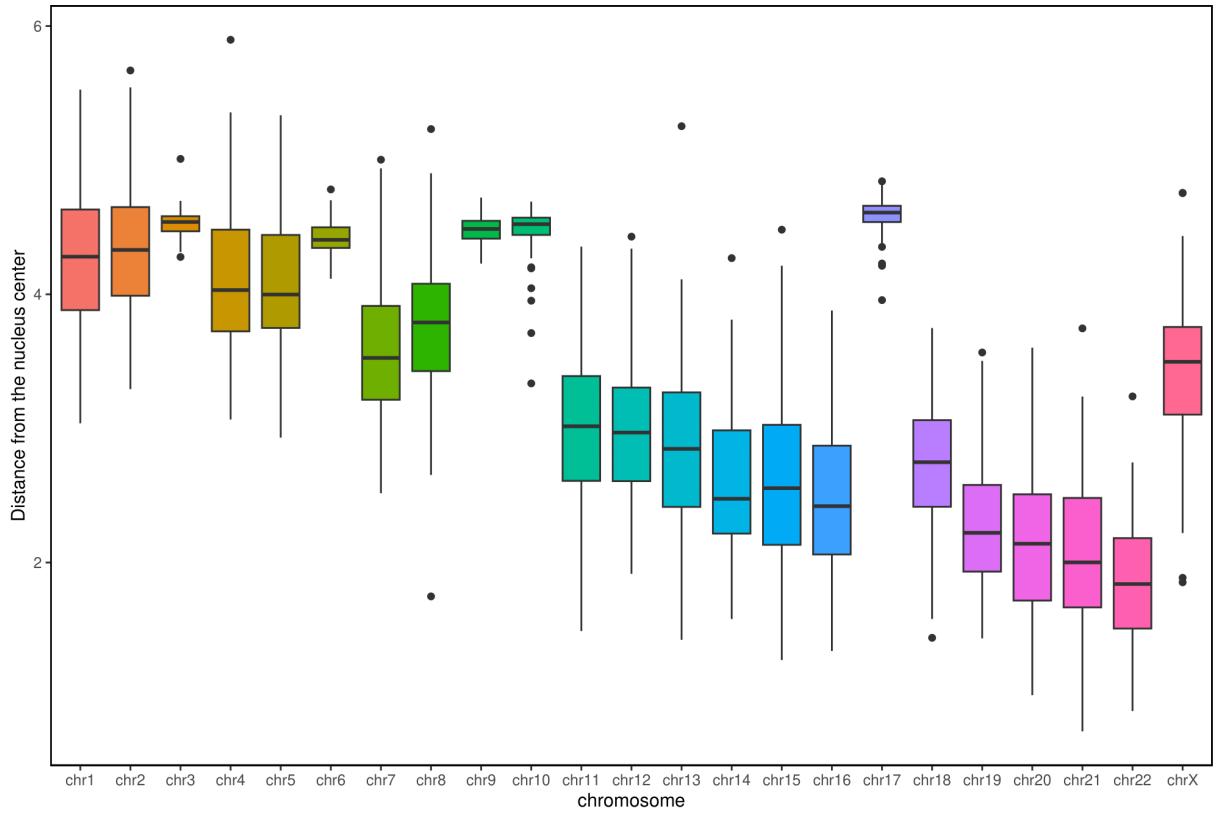

Fig. S25: Median chromosome distance from the nucleus center in 100 Chrom3D simulation models based on T1.

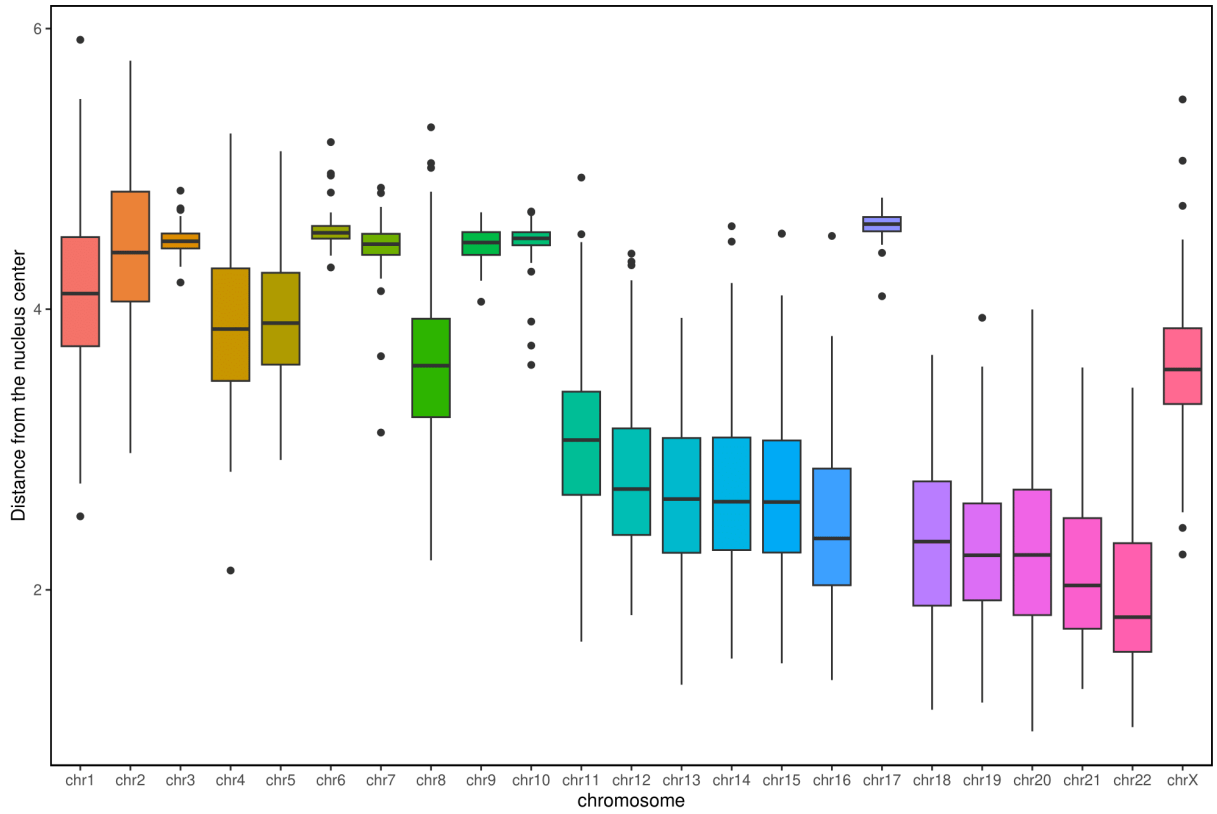

Fig. S26: Median chromosome distance from the nucleus center in 100 Chrom3D simulation models based on C1.

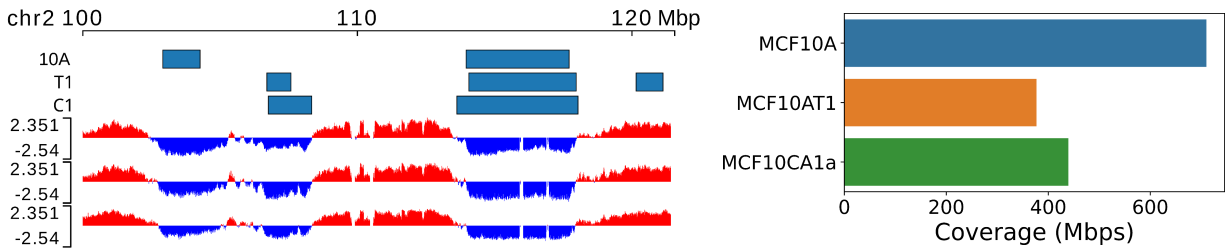

Fig. S27: Coverage of lamina associated domains (LADs).
Left: browser view of a region on Chromosome 2 showing LMNB1 LADs for MCF10A (WT), MCF10AT1 (T1) and MCF10CA1a (C1) as blue bars. Principal component 1 for the same cell lines is shown below. Regions corresponding to A and B compartments are colored in red and blue respectively. Right: Genome-wide coverage of lamina associated domains.

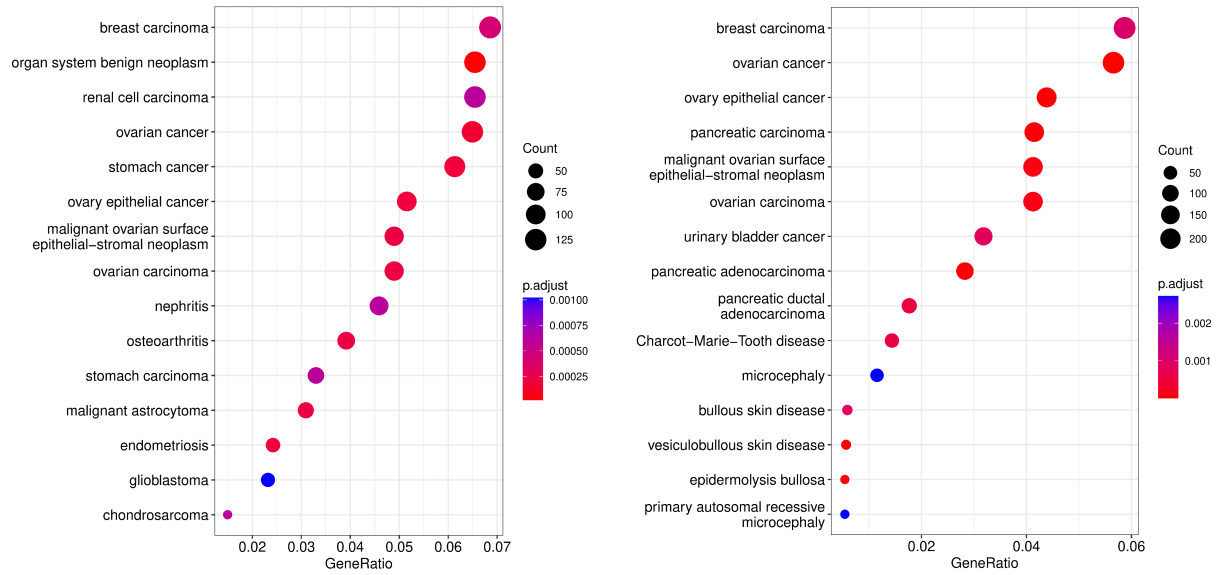

Fig. S28: Over-representation analysis for disease ontology (DO) terms for differentially expressed genes in MCF10AT1 (T1) (left) and MCF10CA1a (C1) (right) using MCF10A (10A) as contrast (lfc=0.5, p-value=0.01). Disease terms are sorted by the fraction of differentially expressed genes found in a given gene set. Dot size is proportional to the number of differentially expressed genes found in a given gene set. Dots are colored based on the statistical significance of the enrichment.

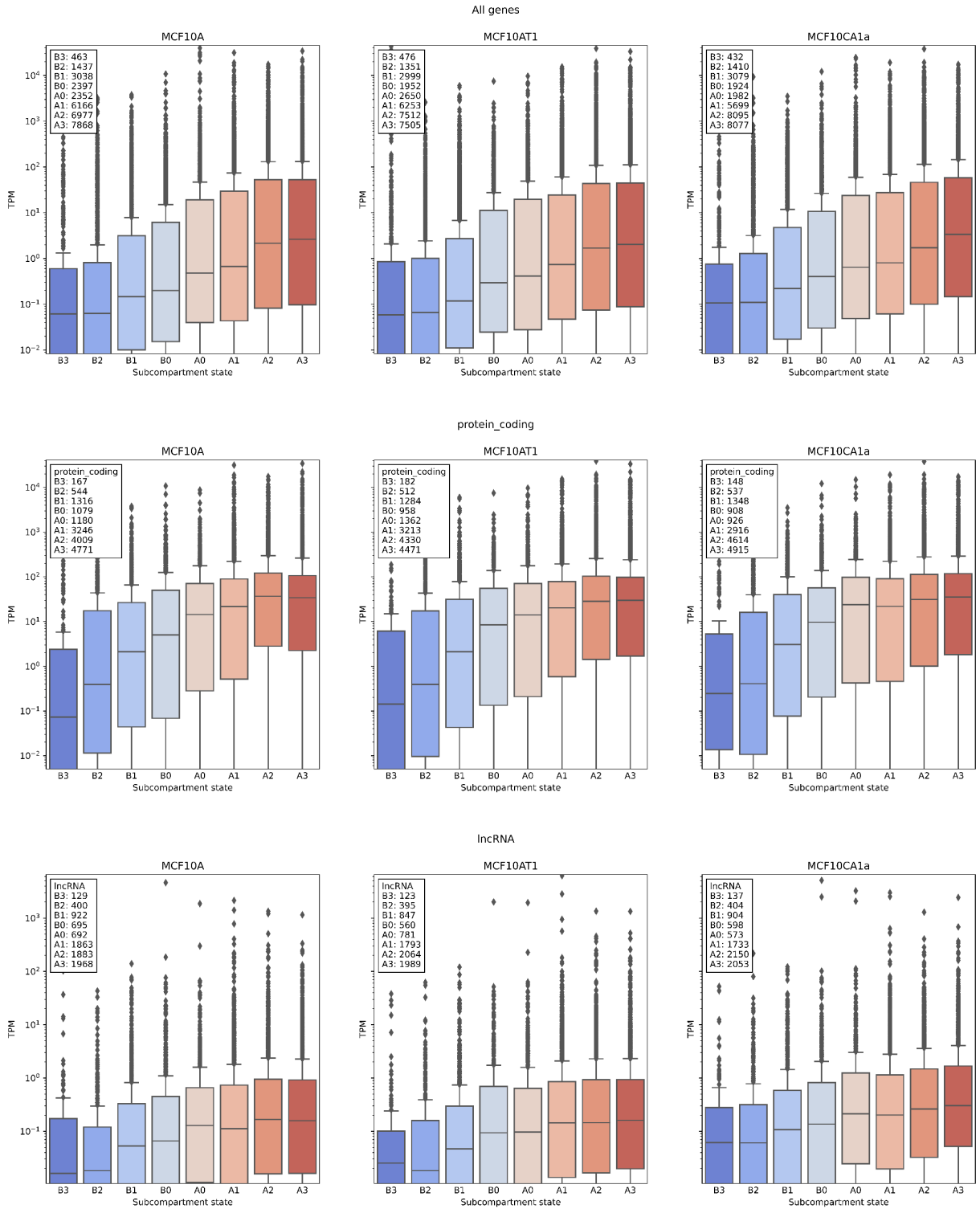

Fig. S29 Distribution of expression levels (TPM) for each subcompartment across MCF10A (left panels), MCF10AT1 (middle panels) and MCF10CA1a (right panels). Rows 1 to 3 show the expression level for all genes, genes encoding for proteins, and long non-coding RNA, respectively. Legend shows the number of genes expressed in each subcompartment.

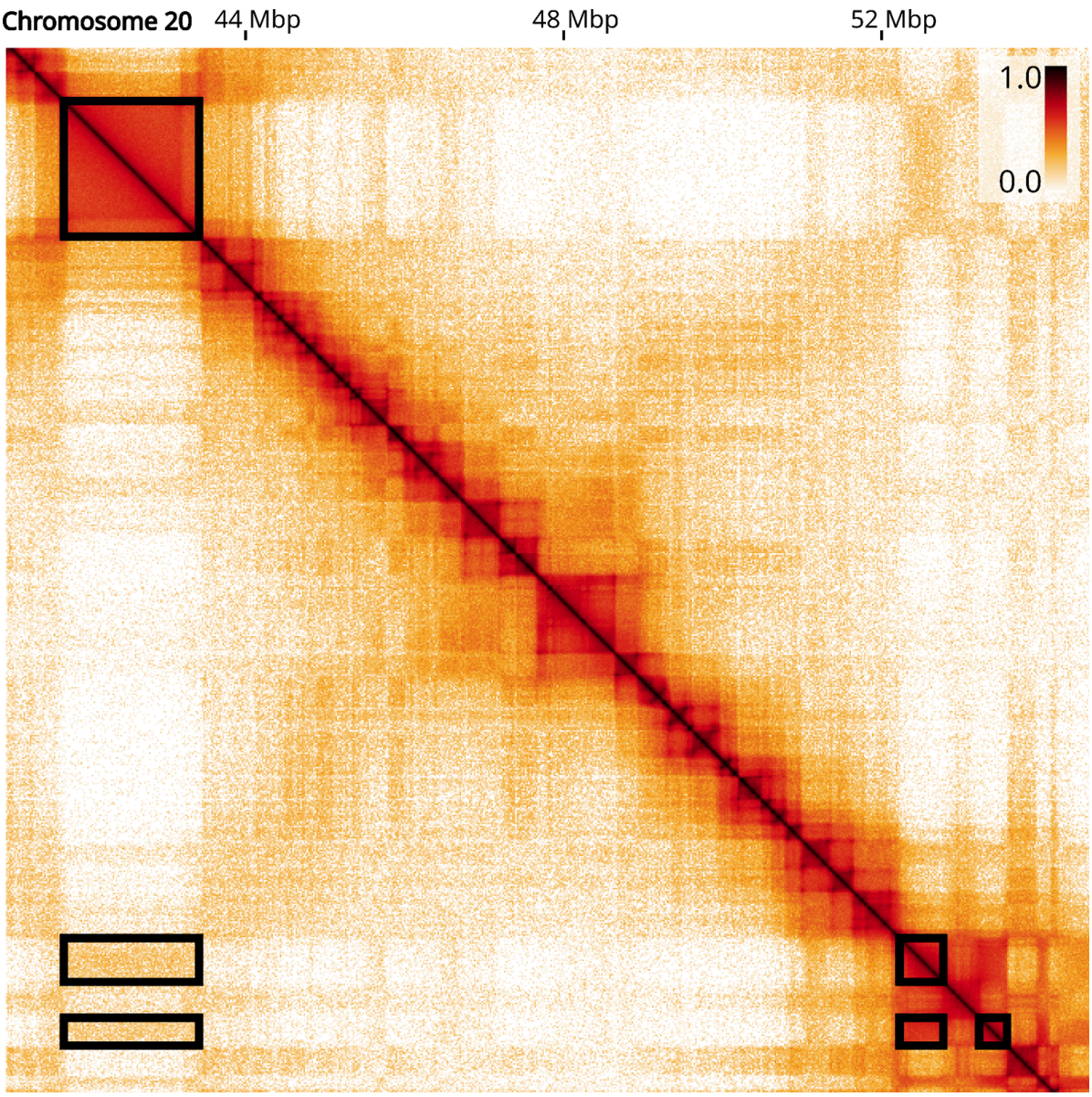

Fig S30: Hi-C matrix showing an example of a TAD clique of size 3. Domains involved in the TAD clique are enclosed in black rectangles.

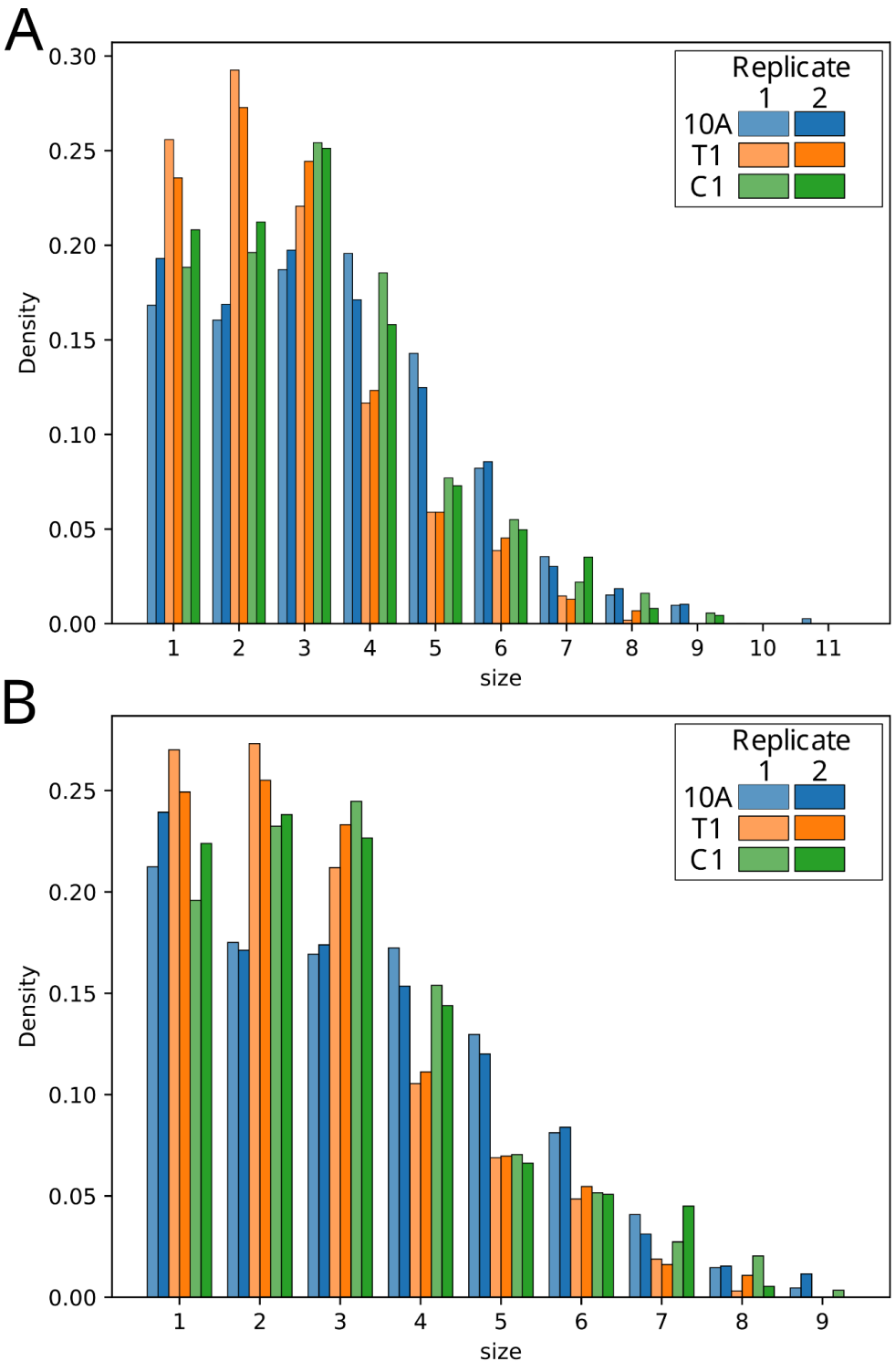

Fig. S31: **A** Bar plot showing the distribution of maximal clique sizes for MCF10A, MCF10AT1 and MCF10CA1a. Heights of bars are normalized such that bars for each replicate sum up to 1. **B** Bar plot showing the same data as panel A after masking cliques with one or more TADs overlapping with regions that are involved in translocation events in any of the 3 cell types studied.

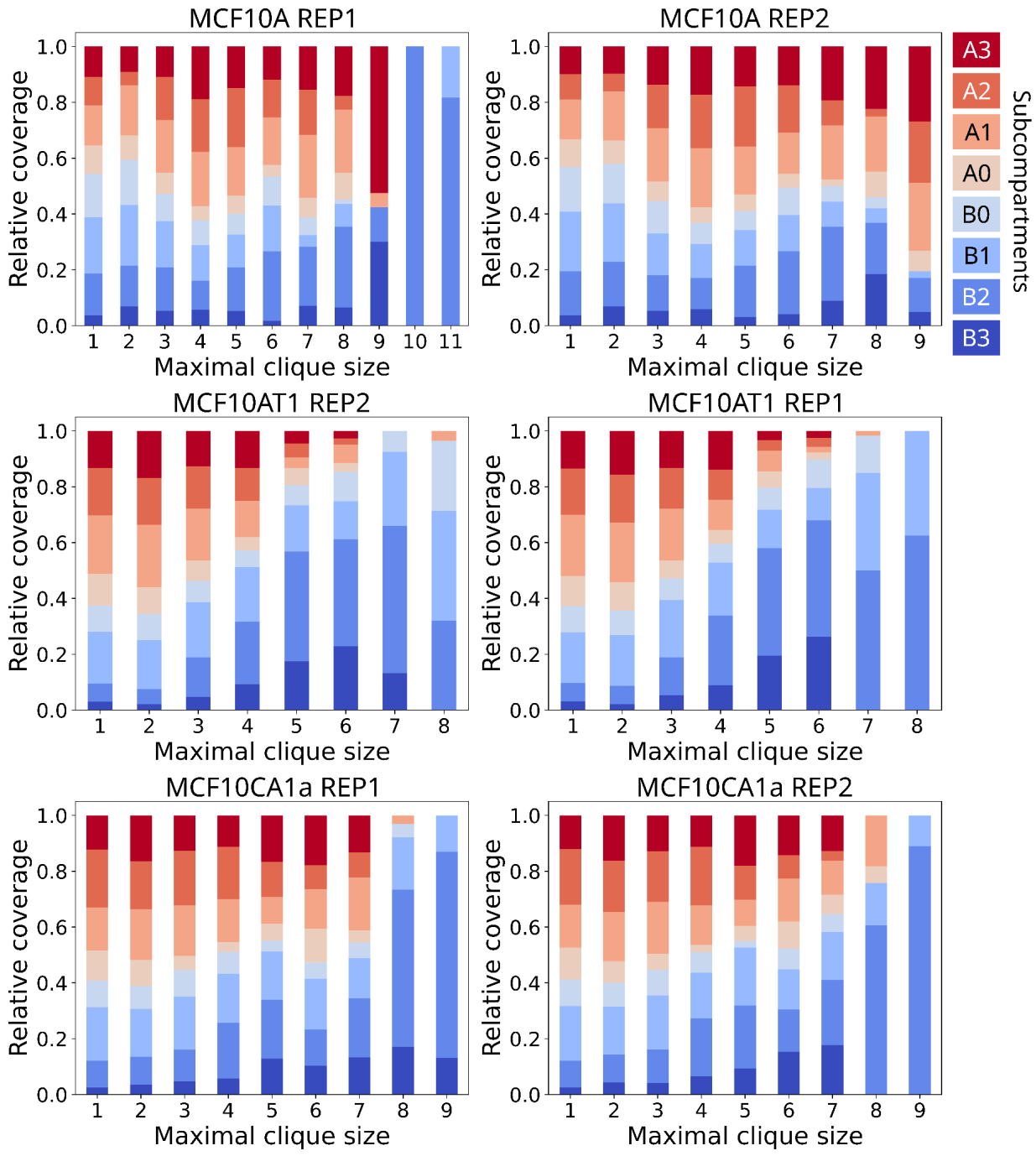

Fig. S32: Subcompartment composition of TAD cliques of size 1-11 in 10A (first row), T1 (second row) and C1 (third row). Cliques of size 1 and 2 are composed of singleton and binary TAD interactions not belonging to any clique.

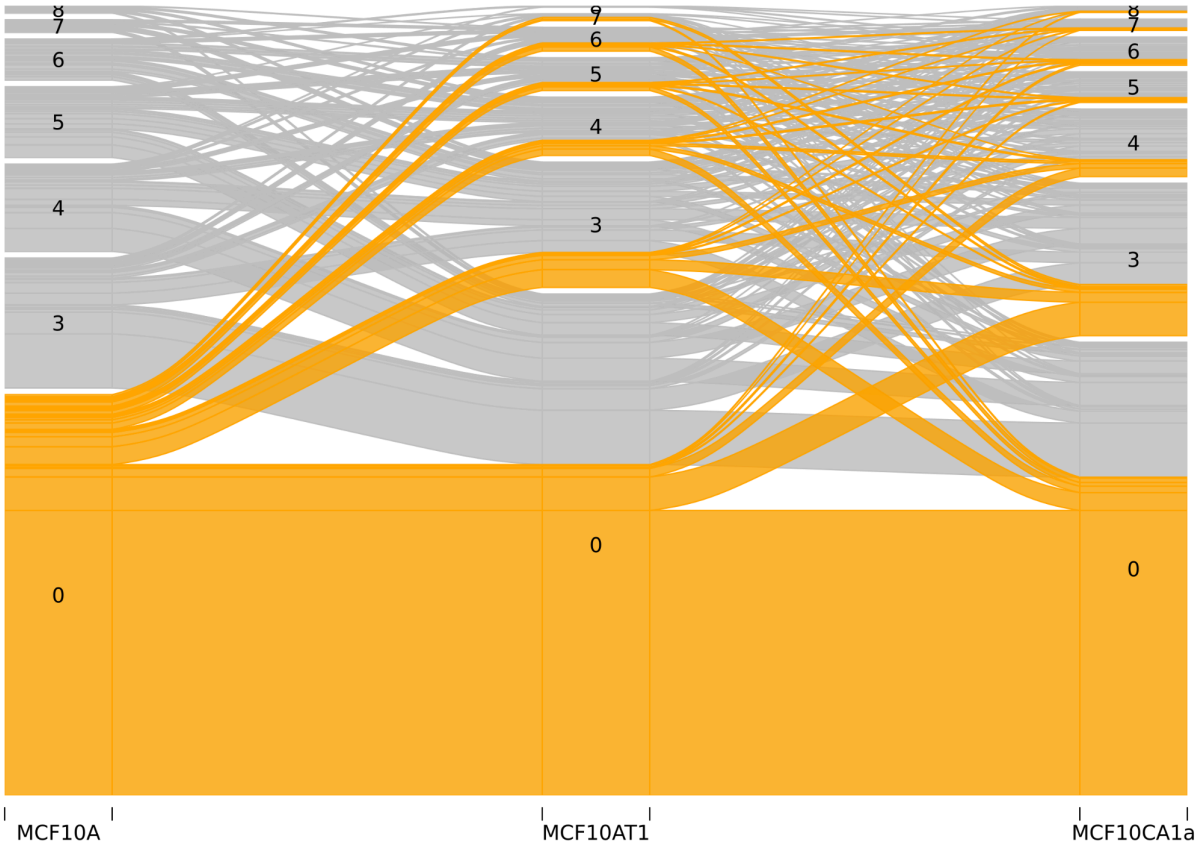

Fig. S33: Alluvial plot showing changes in TAD maximal clique size across the three cancer stages. The orange color highlights the alluvial path that starts with a non-clique (denoted as 0) in MCF10A (10A).

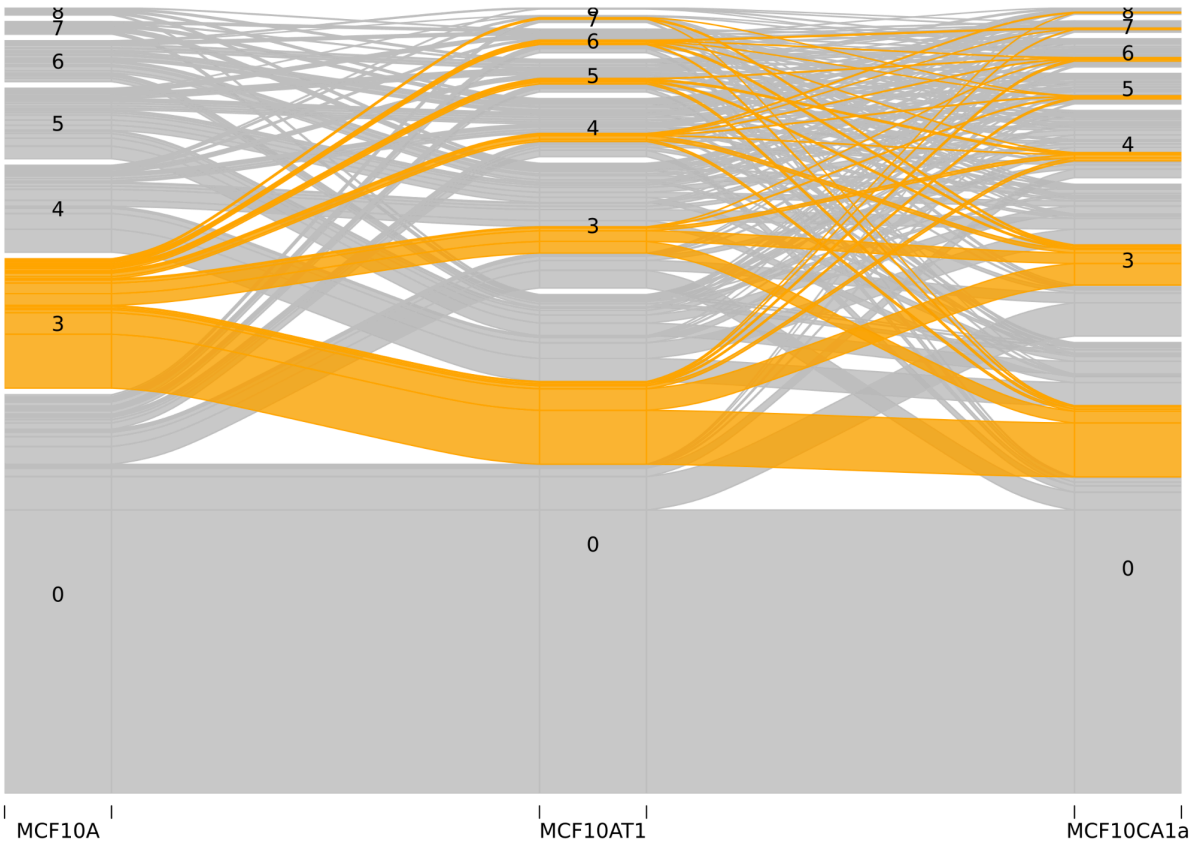

Fig. S34: Alluvial plot showing changes in TAD maximal clique size across the three cancer stages. The orange color highlights the alluvial path that starts with a clique of size 3 in MCF10A (10A).

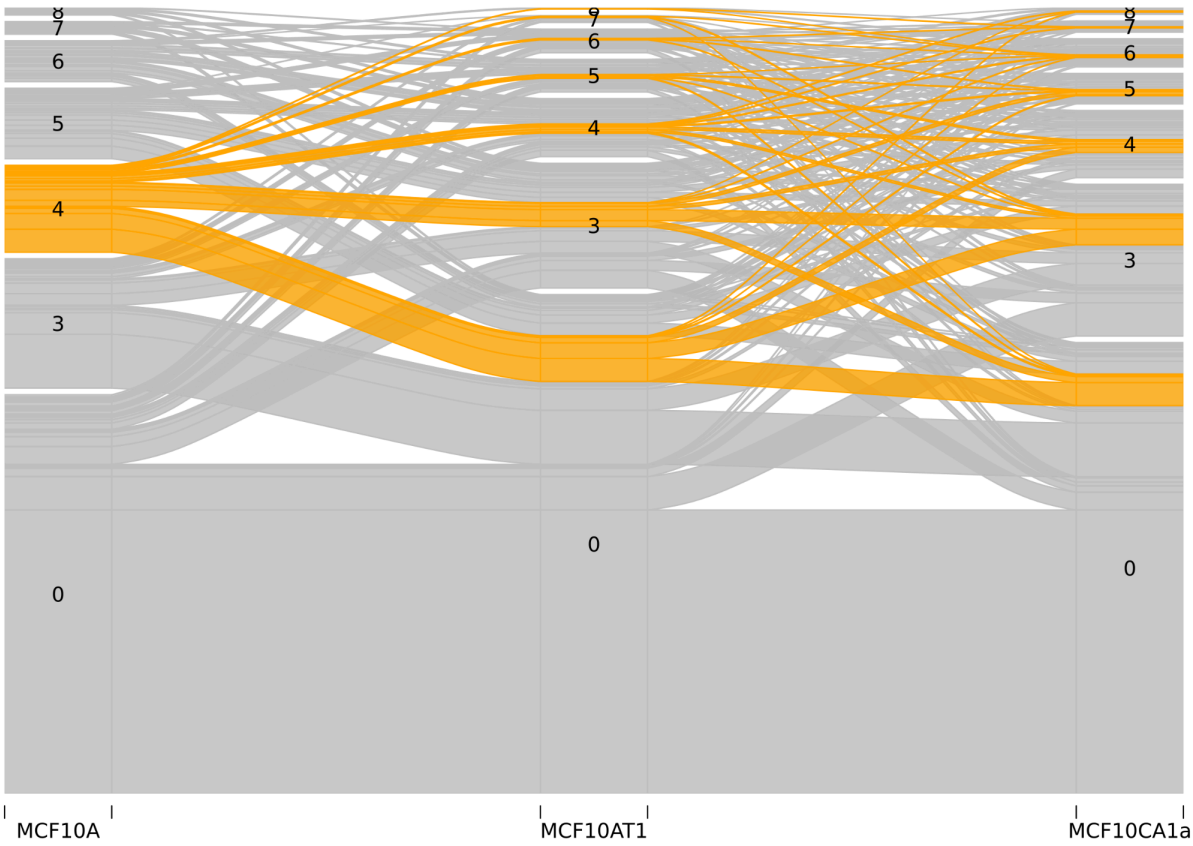

Fig. S35: Alluvial plot showing changes in TAD maximal clique size across the three cancer stages. The orange color highlights the alluvial path that starts with a clique of size 4 in MCF10A (10A).

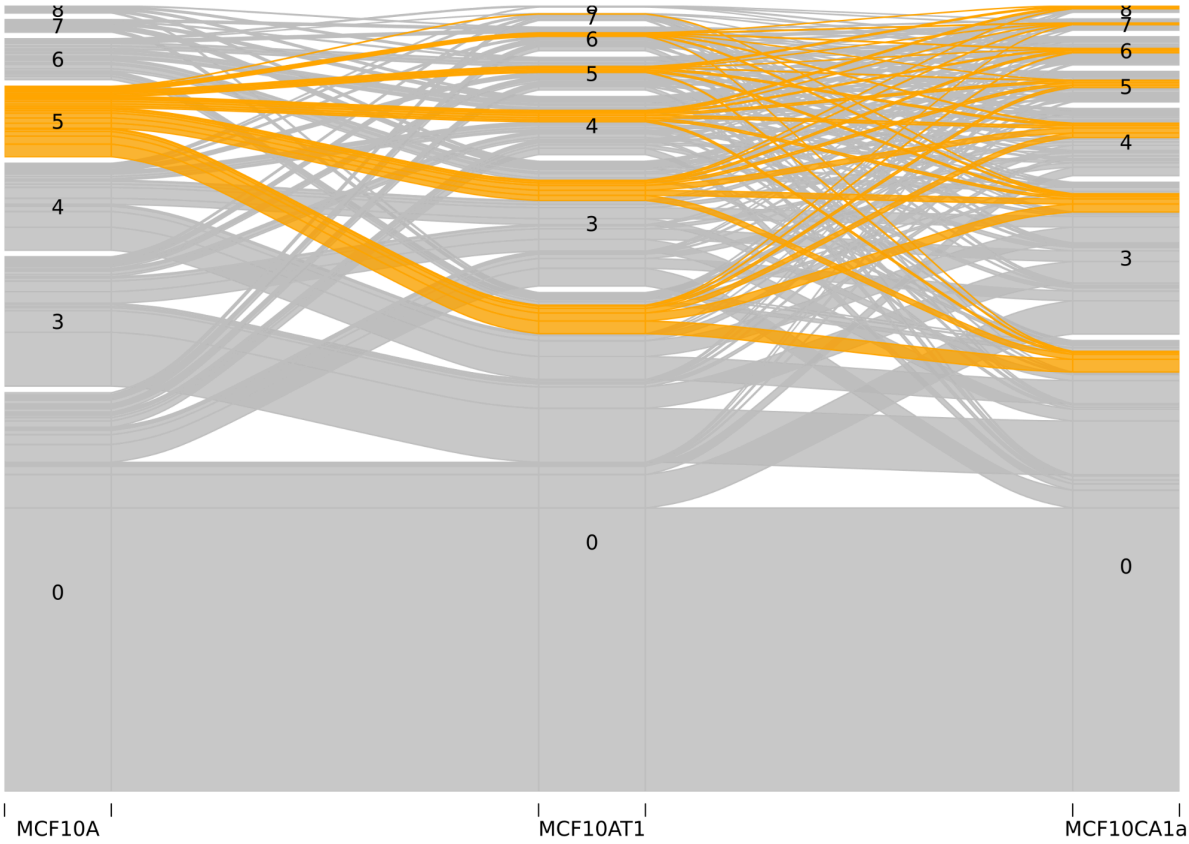

Fig. S36: Alluvial plot showing changes in TAD maximal clique size across the three cancer stages. The orange color highlights the alluvial path that starts with a clique of size 5 in MCF10A (10A).

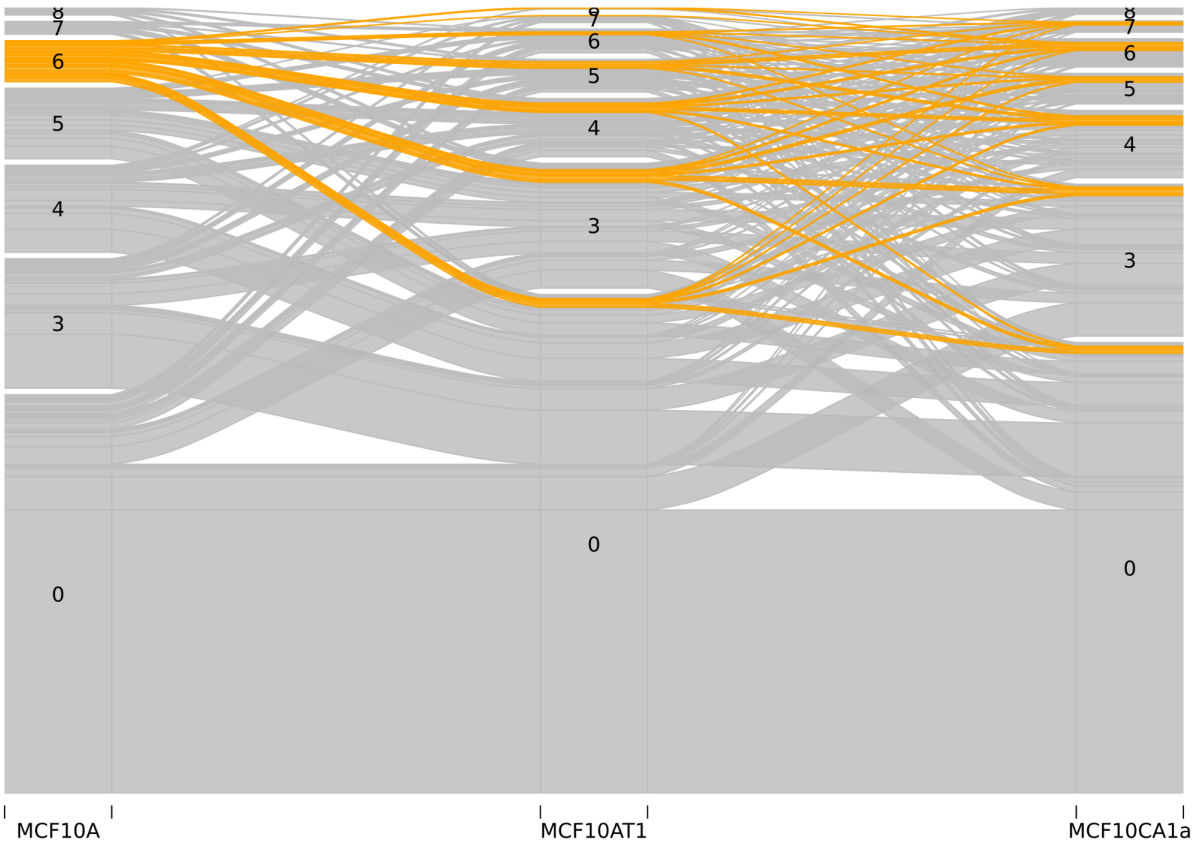

Fig. S37: Alluvial plot showing changes in TAD maximal clique size across the three cancer stages. The orange color highlights the alluvial path that starts with a clique of size 6 in MCF10A (10A).

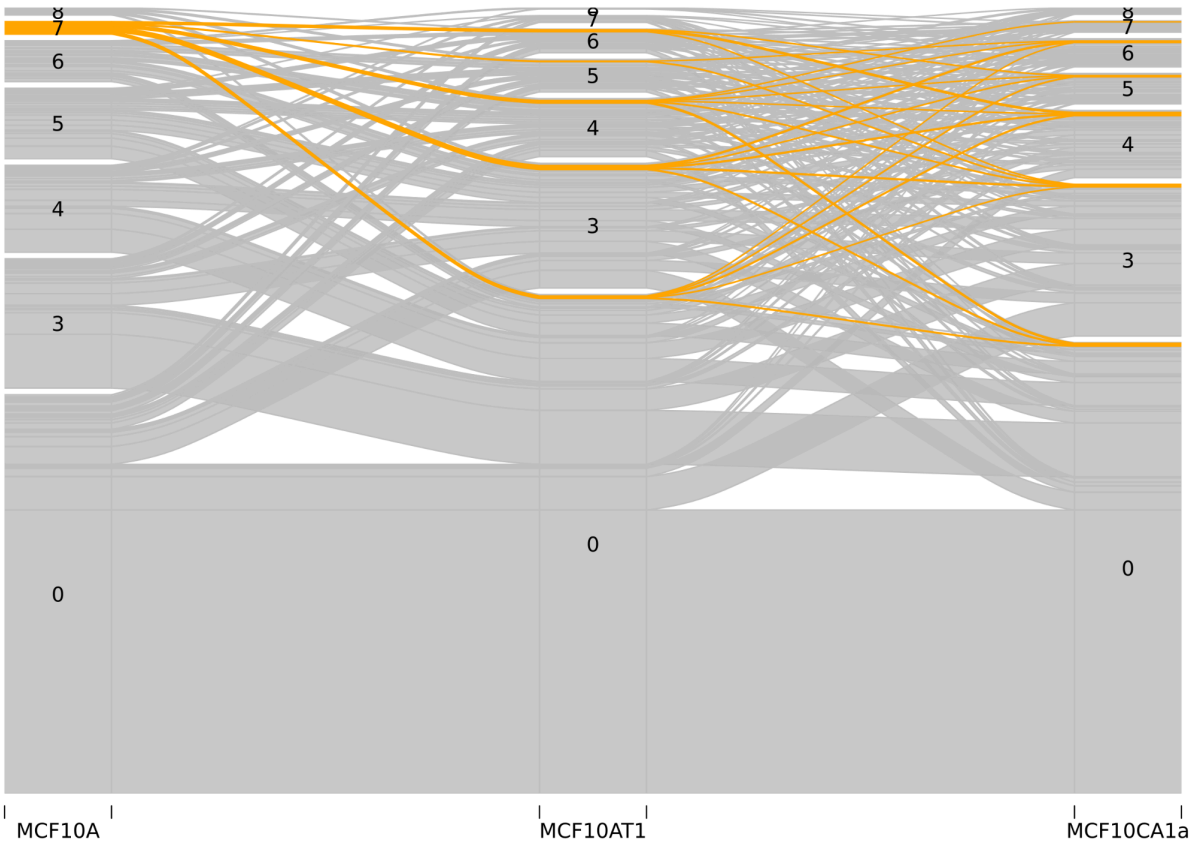

Fig. S38: Alluvial plot showing changes in TAD maximal clique size across the three cancer stages. The orange color highlights the alluvial path that starts with a clique of size 7 in MCF10A (10A).

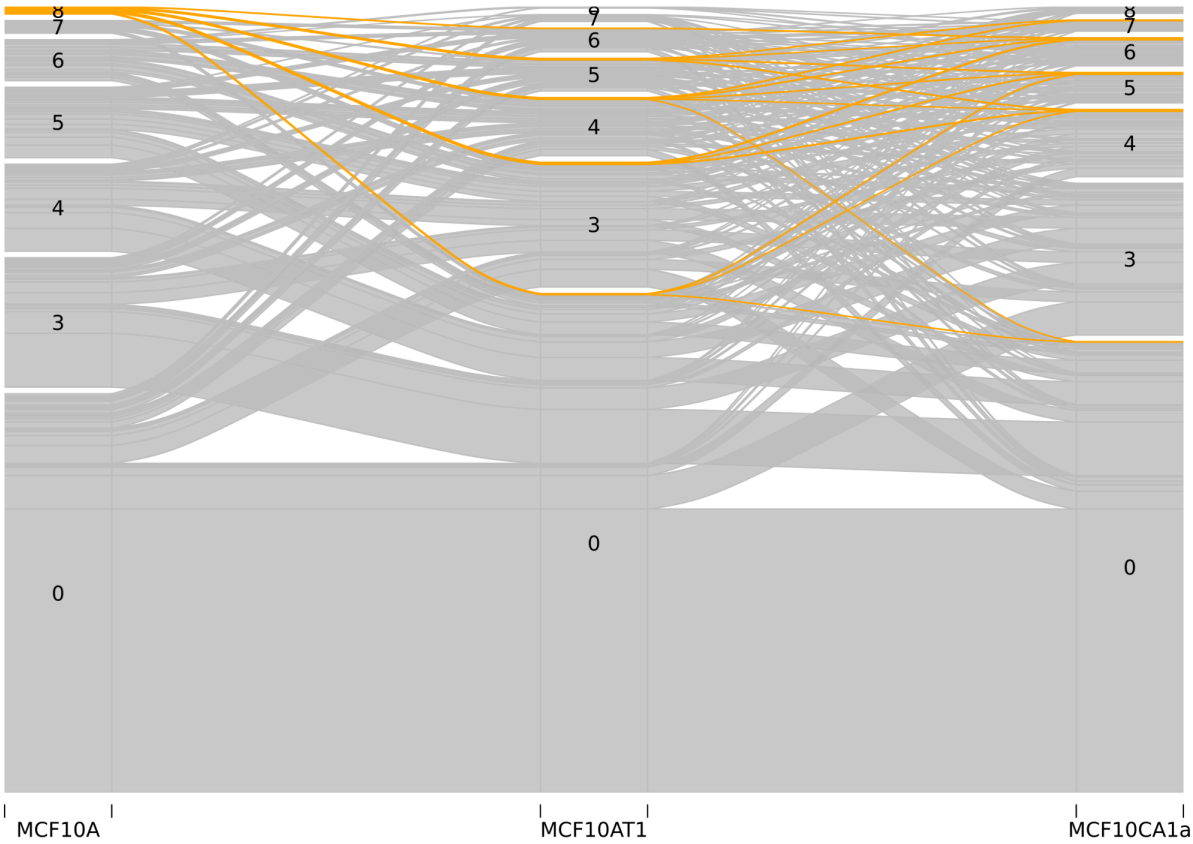

Fig. S39: Alluvial plot showing changes in TAD maximal clique size across the three cancer stages. The orange color highlights the alluvial path that starts with a clique of size 8 in MCF10A (10A).

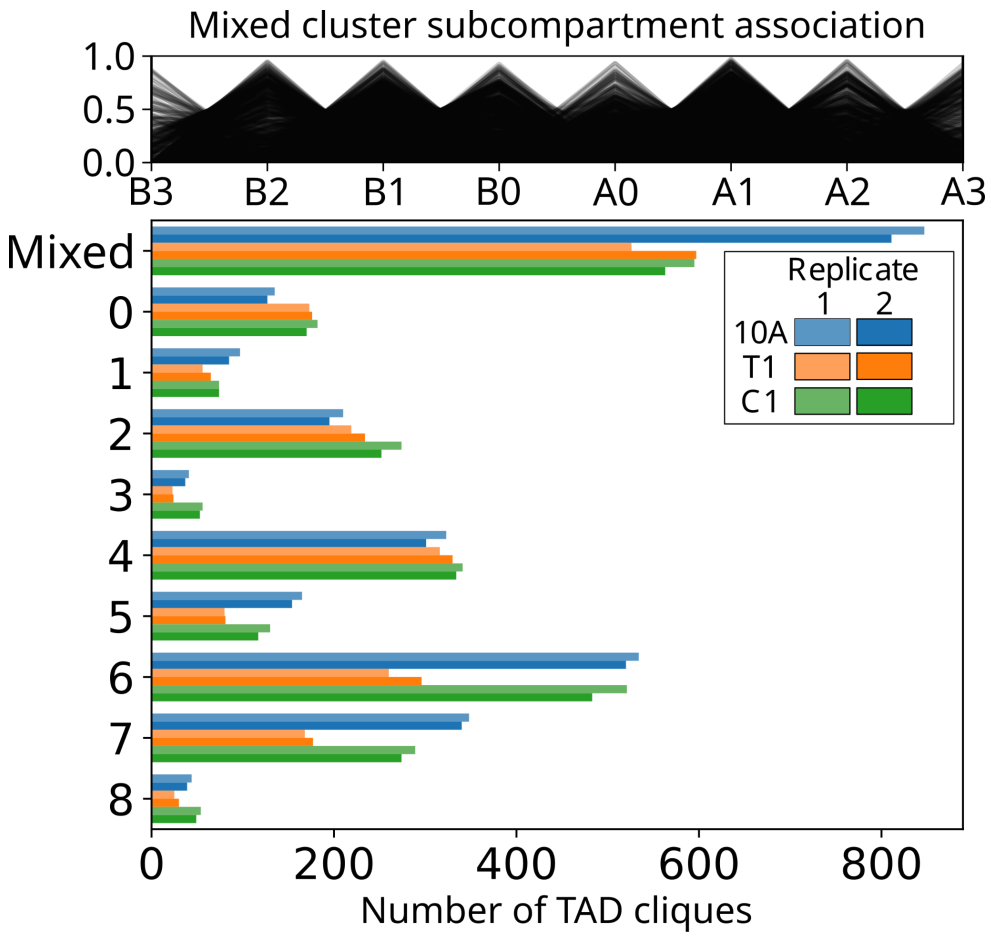

Fig. S40: A: Subcompartment enrichment for TAD cliques placed in the outlier (“mixed”) cluster by HDBSCAN. **B**: Cluster sizes for TAD clique clusters shown in Fig. 3F (including the mixed cluster).

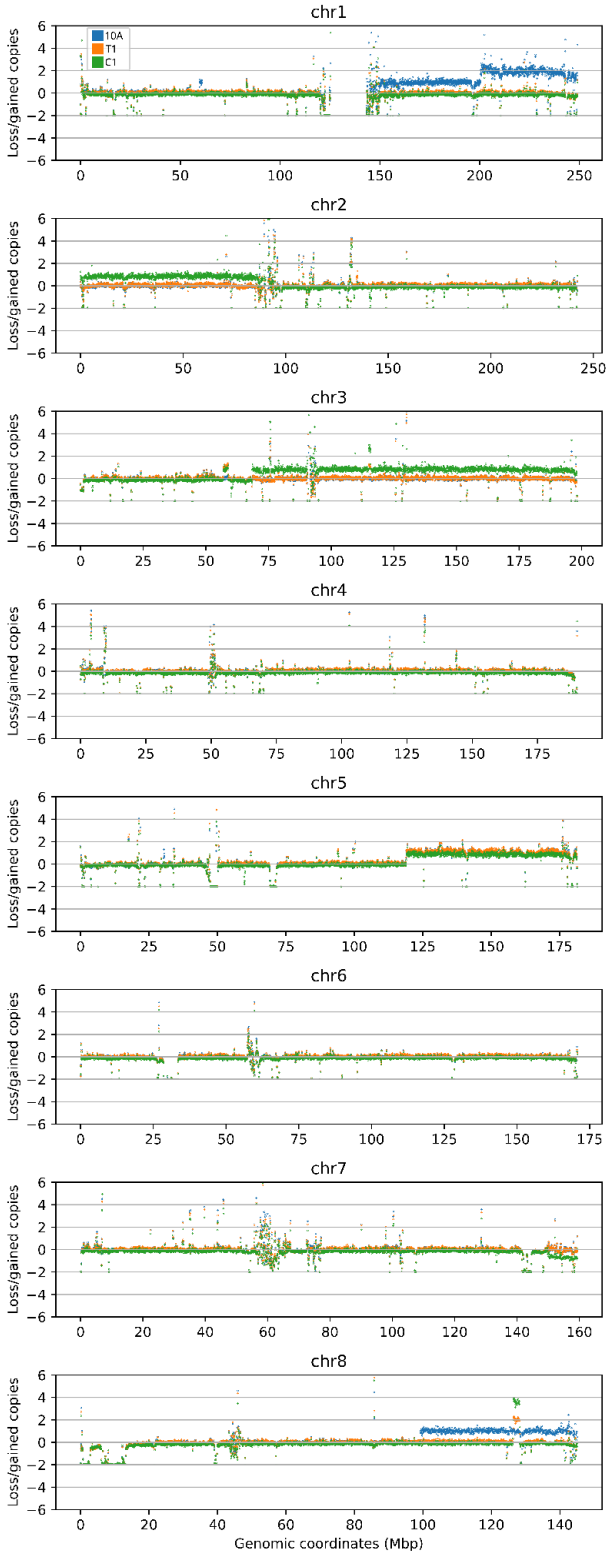

Fig. S41: Figure showing called CNVs across genome. Chrs 1-8

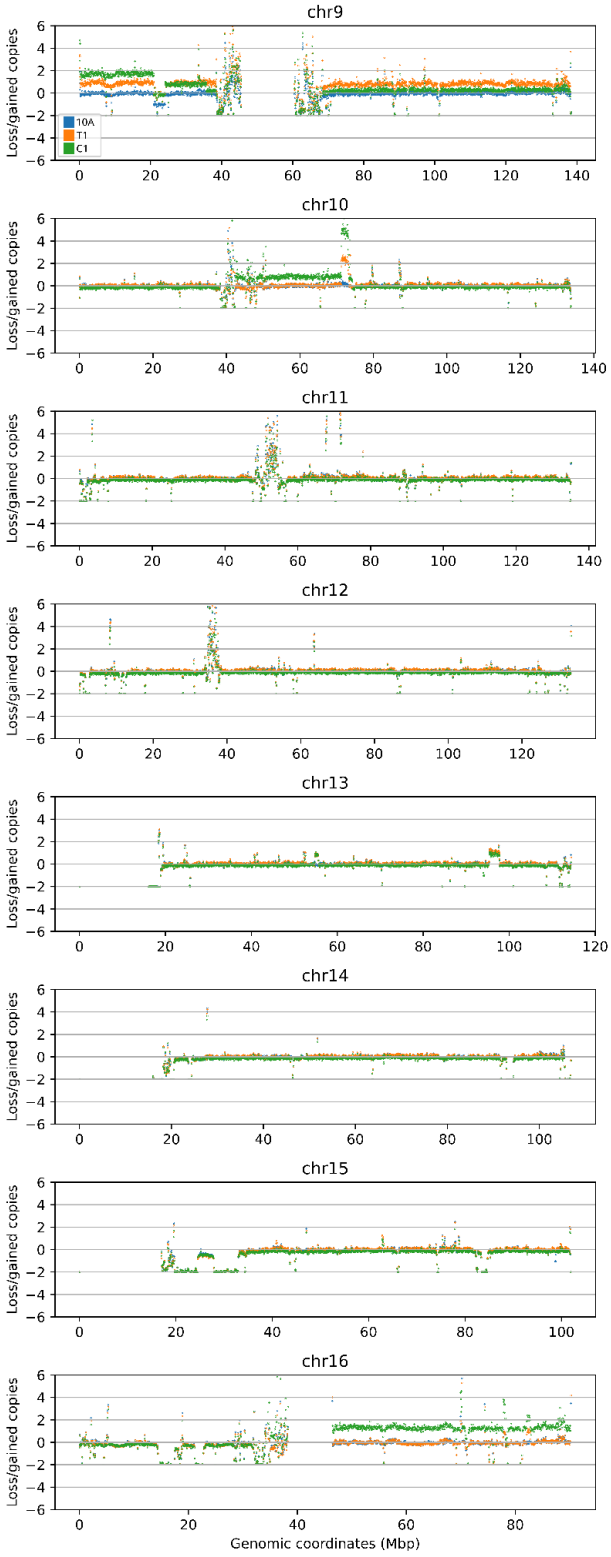

Fig. S42: Figure showing called CNVs across genome. Chrs 9-16

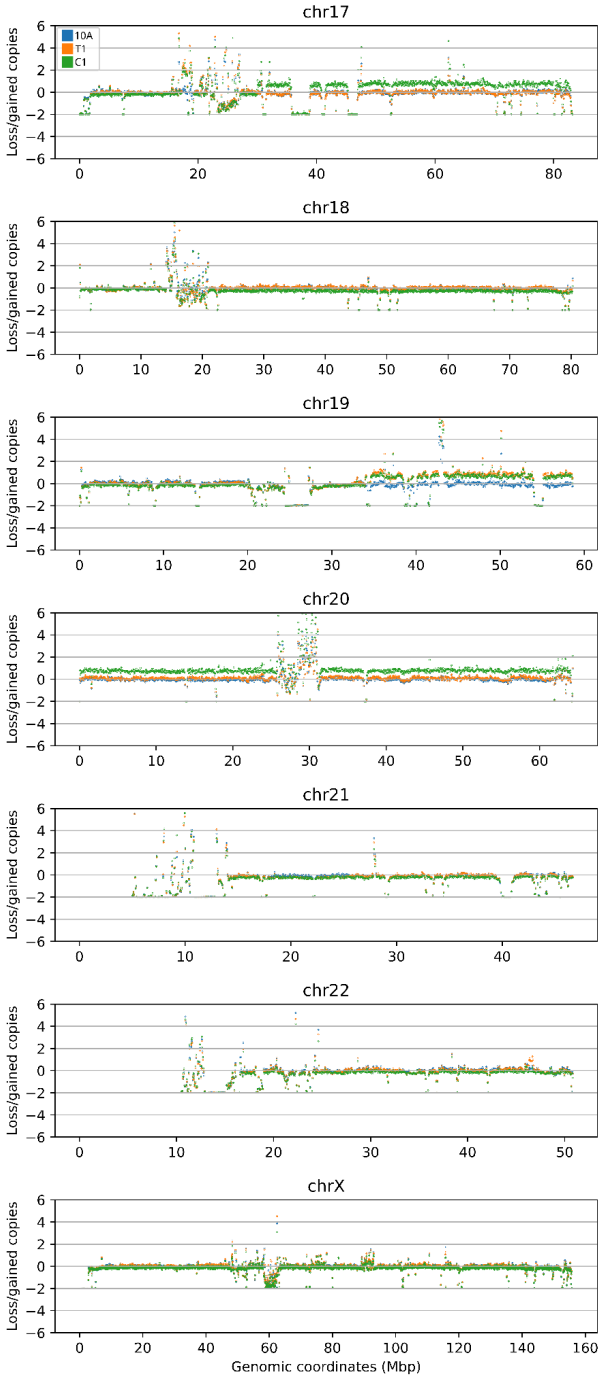

Fig. S43: Figure showing called CNVs across genome. Chrs 17-X

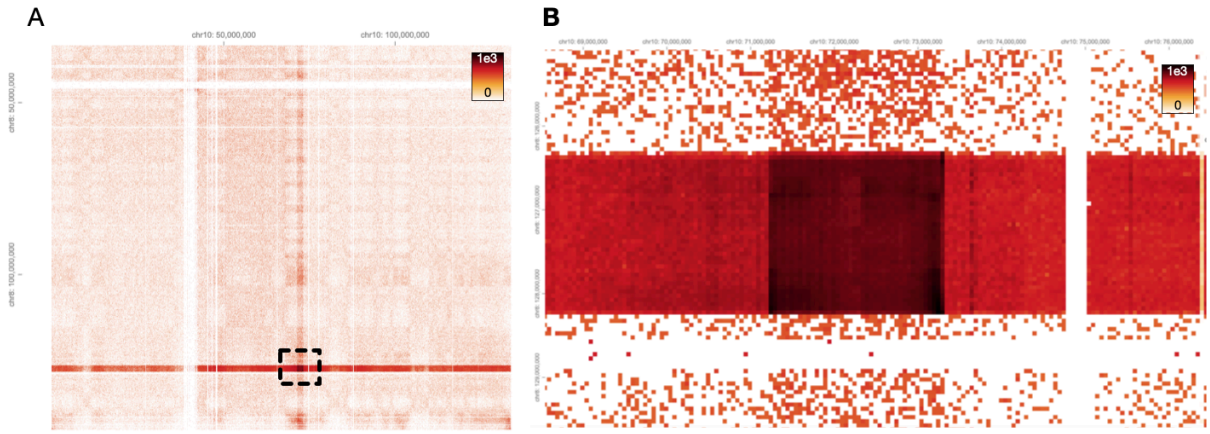

Fig. S44: **A**: Hi-C contact patterns (50 kbp bin resolution) in the genome region surrounding the *MYC*-insertion region on Chromosome 8 (vertical axis) and Chromosome 10 (horizontal axis) in C1 cells using the LOcal Iterative Correction (LOIC) balancing scheme, which takes copy number alterations into account (see Methods)]. **B**: Zoom-in on the *MYC*-insertion region, showing enriched contacts between regions on 8 (126330000-128235000 bp; hg38) and Chromosome 10 (71280000-73310000 bp; hg38).

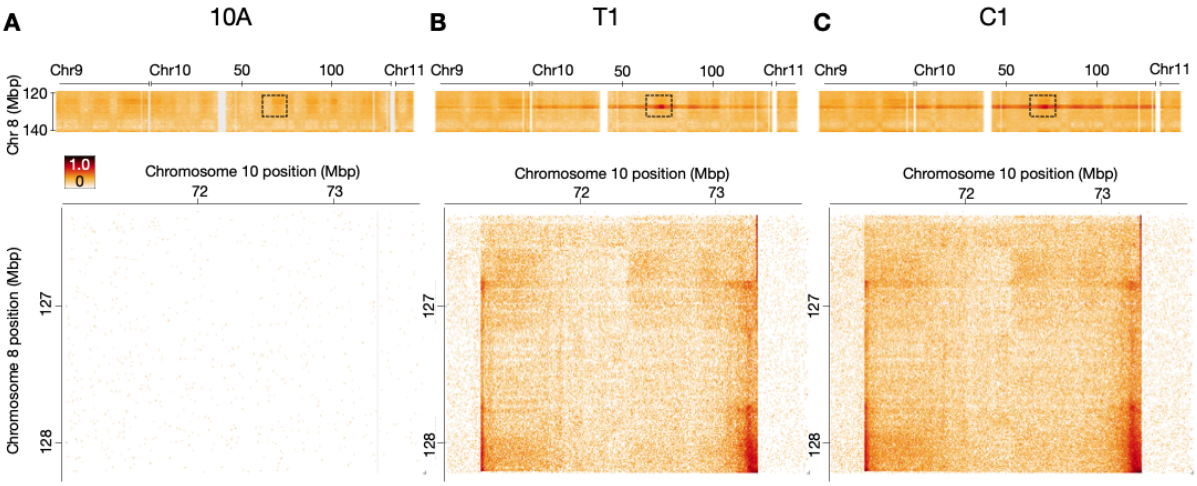

Fig. S45: **A**: Top: Interchromosomal 10A Hi-C contacts between the region on Chromosome 8 (vertical axis) and the entire Chromosome 10. End of Chromosome 9 and beginning of Chromosome 11 shown on the left and right side, respectively. The dotted square highlights the *MYC* insertion region. Bottom: Zoom-in on the 10A Hi-C map of the Chromosome 8/10 amplification unit, showing lack of contact enrichment in this region **B**: As in A, but showing contacts for T1. The bottom panel shows extensive Hi-C interactions indicating presence of the insertion region. **C**: As in A, but showing contacts for C1. The bottom panel shows extensive Hi-C interactions indicating presence of the insertion region

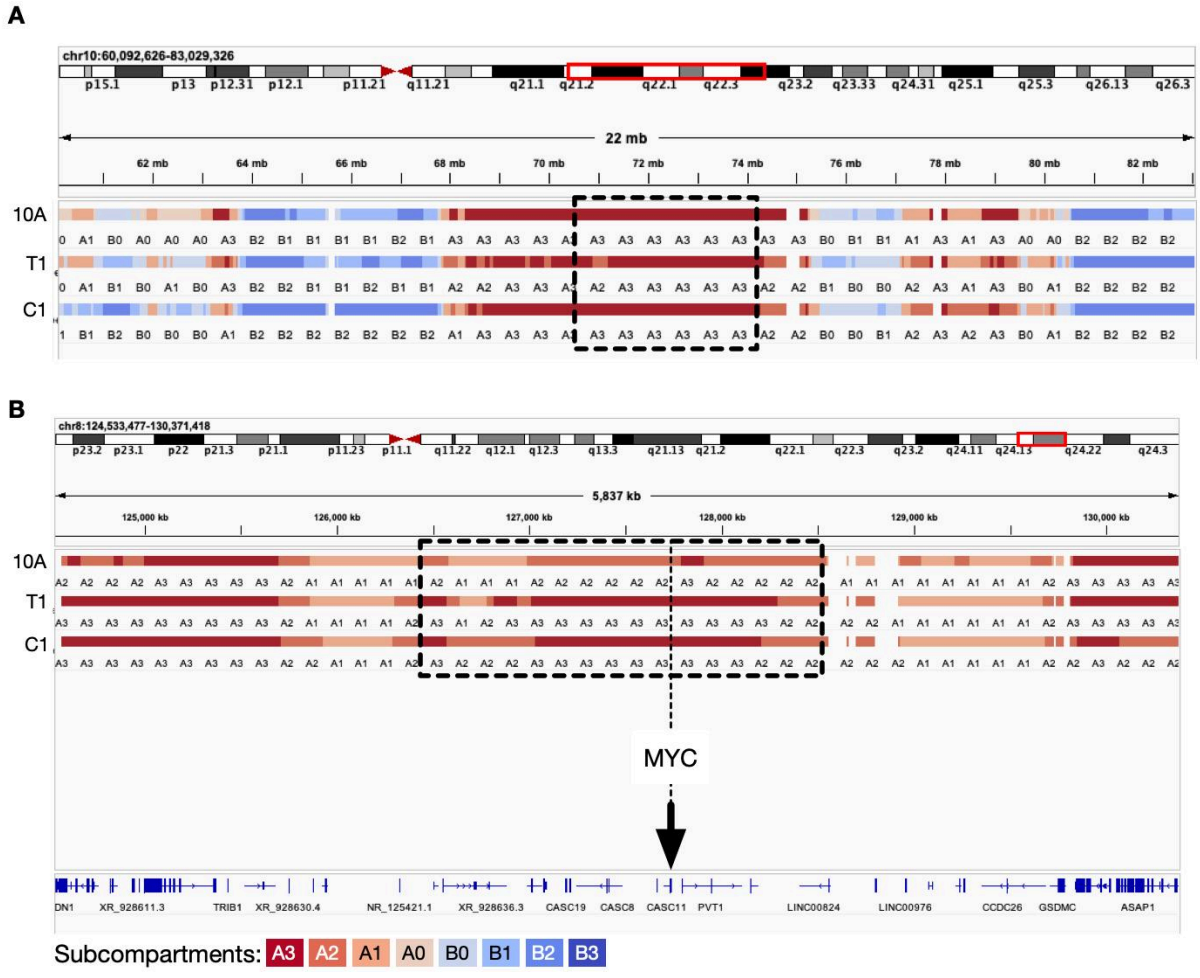

Fig S46: **A**: Genome browser view of subcompartments surrounding and including the amplified region in the three cell types on Chromosome 10 (dotted lines) **B:** Genome browser view of subcompartments in the three cell types surrounding and including the amplified region on Chromosome 8 (dotted lines).

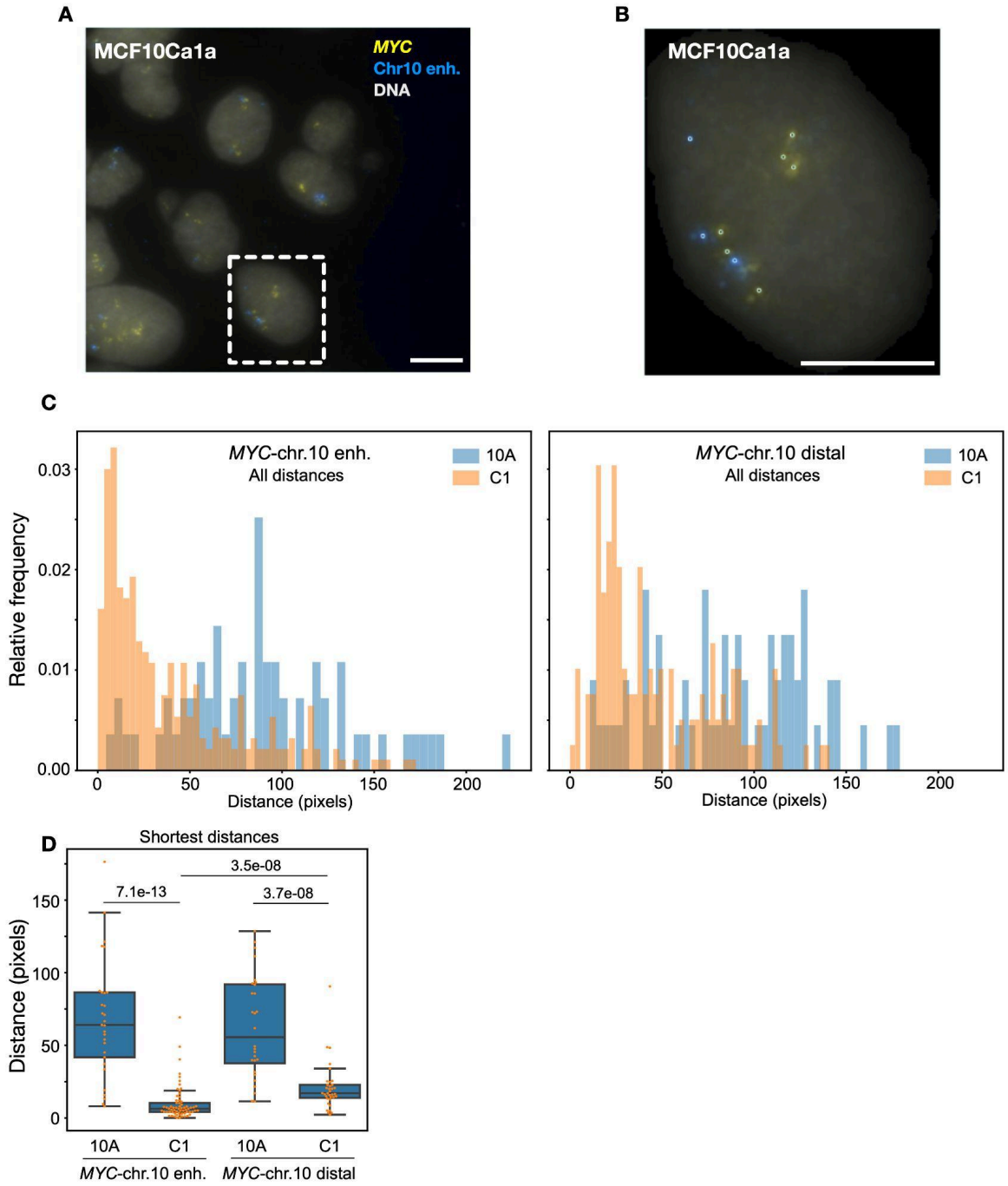

Fig S47: **A**: FISH image of the *MYC* gene (yellow) and the Chromosome 10 enhancer (blue; Chr.10 position 73117711-73267436) in C1 cells. **B**: Zoom-in on the region highlighted in A (dotted square). Bars, 7 µm. **C**: Left: Distribution of all distances (pixels) between the *MYC* gene and the enhancer probe in 10A (blue) and C1 (orange). Right: distribution of all distances (pixels) between the *MYC* gene and a downstream non-enhancer probe in 10A (blue) and C1 (orange). **D**: Quantification of shortest distance between the *MYC* probe and the nearest probe (either enhancer probe, or distal non-enhancer probe). P-values are shown (Kolmogorov-Smirnov test).

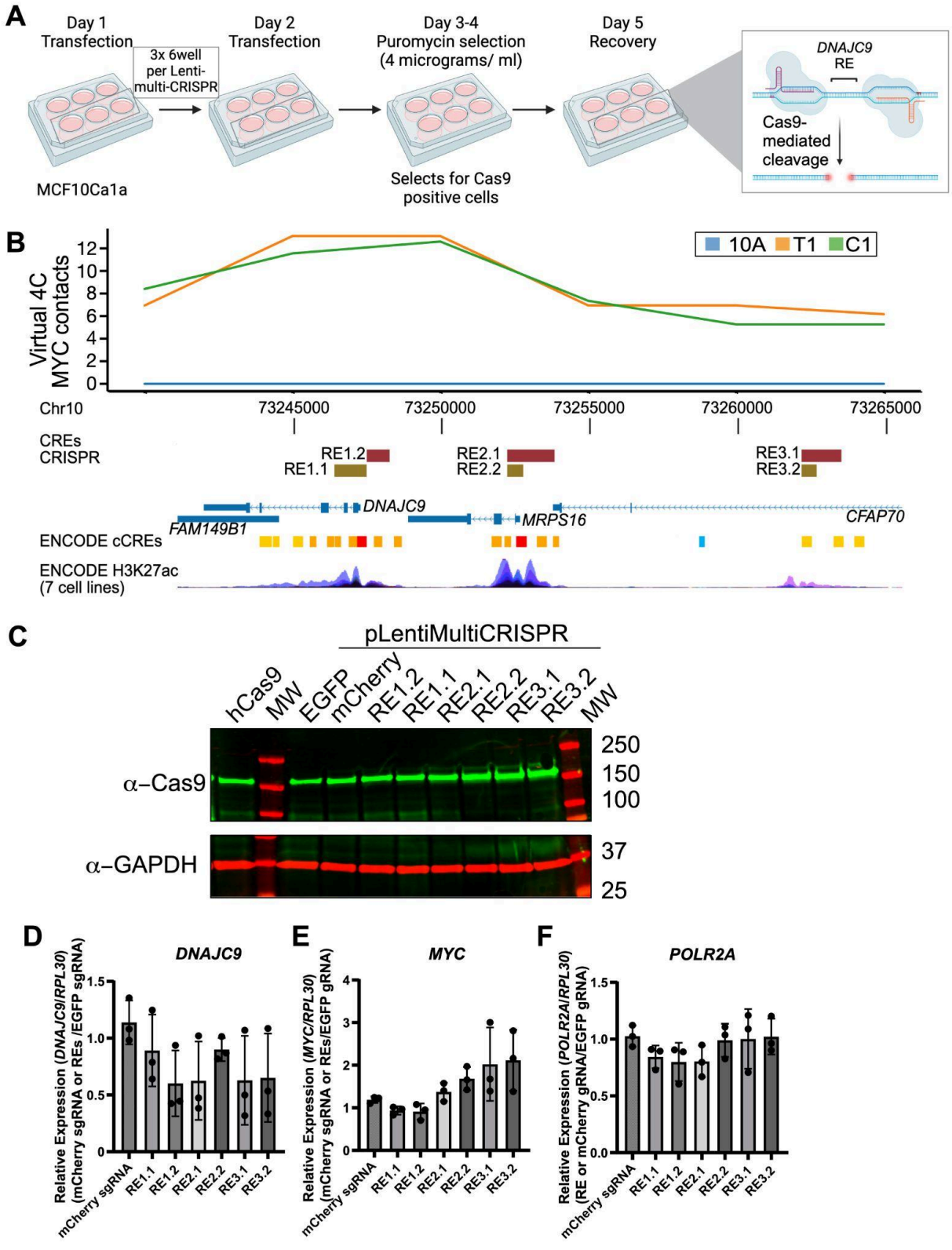

Fig S48: **A:** Overview of CRISPR-Cas9 targeted deletion time-course in C1 cells with sgRNAs targeting three putative regulatory (REs) in the *DNAJC9* locus on Chromosome 10 and two

control sgRNAs targeting mCherry and EGFP. Each pair of sgRNAs combined with Cas9 P2A puromycin in LentiMultiCRISPR (addgene #85402) was transfected with lipofectamine in 3 six-wells and the transfection was repeated after 24 hours. The transfected C1 cells were selected with media containing puromycin for two days and left to recover for one day before collection for RNA and gDNA. Figure created with Biorender.com. **B**: A genomic track (UCSC_hg38) exhibiting ENCODE Cis-Regulatory Elements and layered H3K27 acetylation (H3K27ac) in the human *DNAJC9* locus on Chromosome 10. Selected candidate regulatory elements (RE1, RE2 and RE3) targeted with two sets of pairs of sgRNAs in C1 are indicated by red/brown bars. **C**: Western blot for Cas9 and GAPDH from whole cell extract in C1 pool cells transfected with LentiMultiCRISPR with guide pairs for RE1.1, RE1.2, RE2.1, RE2.2, RE3.1, RE3.2 or guide controls EGFP and mCherry. Expression of humanized Cas9 protein is used as control (addgene #41815). **D**: Relative gene expression analysis of *DNAJC9* upon deletion of candidate regulatory elements (RE1.1, RE1.2, RE2.1, RE2.2, RE3.1 and RE3.2) in the *DNAJC9* locus on Chromosome 10 compared with a control sgRNA for mCherry. *DNAJC9* expression was normalized to the expression of *RPL30*. Relative expression ratio was calculated from pooled cells for each RE deletion and mCherry sgRNA control versus an EGFP sgRNA control. Data are represented as mean +/- STDEV (n=3 different CRISPR-Cas9 time-courses). A one-way ANOVA Dunnett's test between mCherry sgRNA and each of different RE guide pairs was not shown to be significant. **E**: Relative gene expression analysis of *MYC* upon deletion of six REs in the *DNAJC9* locus on Chromosome 10 compared with a control sgRNA for mCherry. *MYC* expression was normalized to the expression of *RPL30*. Relative expression ratio was calculated from pooled cells for each RE deletion and mCherry sgRNA control versus an EGFP sgRNA control. Data are represented as mean +/- STDEV (n=3 different CRISPR-Cas9 time-courses, from average of n=3 technical replicates per time-course). A one-way ANOVA Dunnett's test between mCherry sgRNA and each of different RE guide pairs was not found to be significant. **F**: Relative gene expression analysis of *POLR2A* on Chromosome 17 upon deletion with two pairs of sgRNAs per RE in the *DNAJC9* locus compared with a control sgRNA for mCherry. *POLR2A* expression was normalized to the expression of *RPL30*. Relative expression ratio was calculated from pooled cells for each RE deletion and mCherry sgRNA control versus an EGFP sgRNA control. Data are represented as mean +/- STDEV (n=3 different CRISPR-Cas9 time-courses, from average of n=3 technical replicates per time-course). A one-way ANOVA Dunnett's tests between mCherry sgRNA and each of different RE guide pairs were not found to be significant.

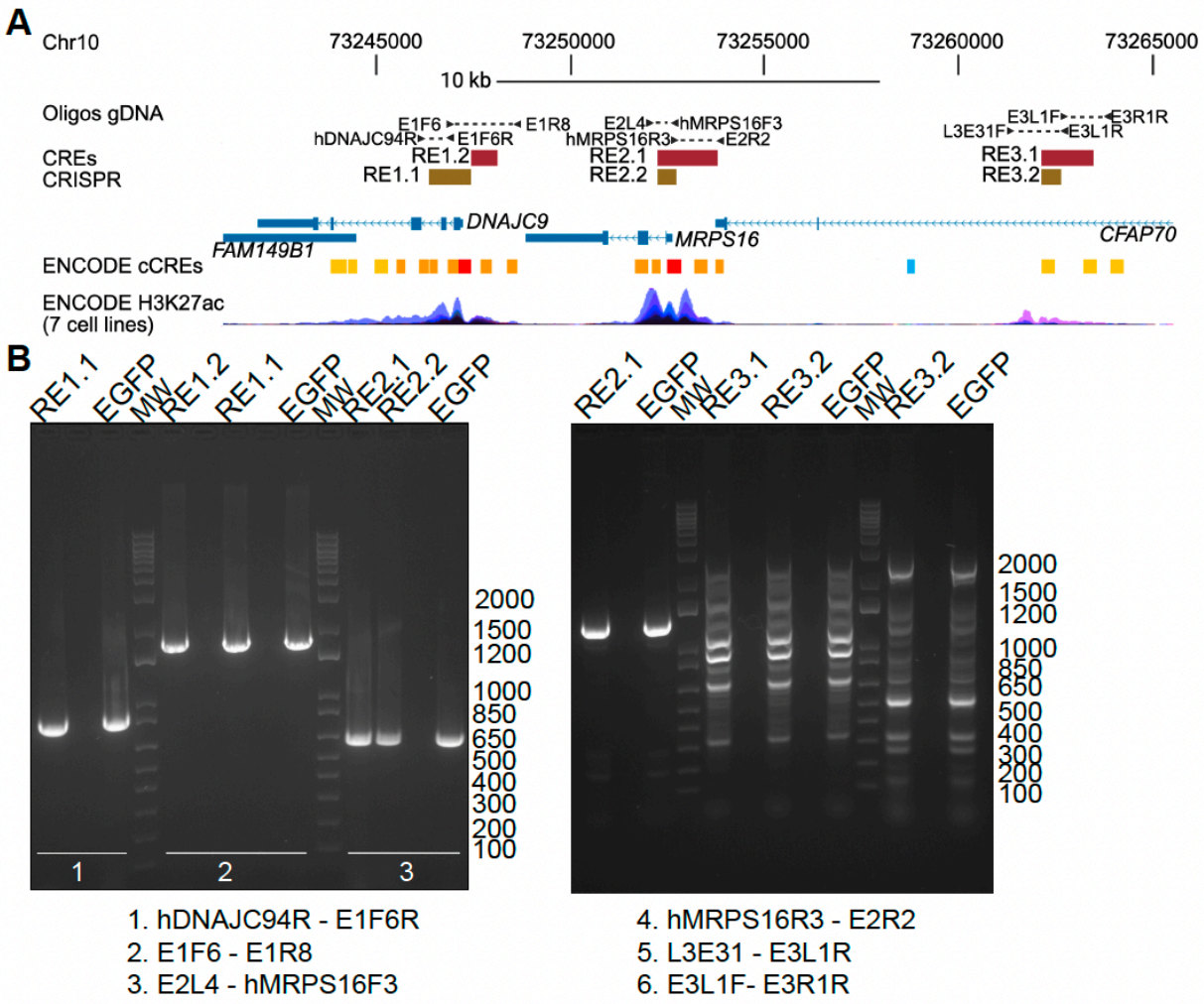

Fig S49: A: A genomic track (UCSC_hg38) exhibiting ENCODE Cis-Regulatory Elements and layered H3K27 acetylation in the human *DNAJC9* locus on Chromosome 10. Oligos used for genomic DNA amplification of regions targeted by gRNA are indicated by forward and reverse arrow and a dashed line for expected PCR product. Selected candidate regulatory elements (RE1, RE2 and RE3) targeted with two sets of pairs of sgRNAs are indicated by red/brown bars. The scale bar is set to 10 kb. Figure created with Biorender.com. **B**: In C1 pool cells transfected twice with LentiMultiCRISPR with sgRNA pairs for RE1.1, RE1.2, RE2.1, RE2.2, RE3.1, RE3.2 or a control EGFP sgRNA pair and selected with puromycin for two days, primer pairs 1-6 were used to span sgRNAs for indel analysis. PCR for RE3 (primer pairs 5 and 6) did not reveal a single band at expected size and was therefore not sequenced. PCR products from primer pairs 1-4 were purified and sent for Sanger sequencing to measure the number of indels surrounding the breakpoint for individual sgRNAs using the TIDE webtool.